THE EFFECT OF NOSE RADIUS ON THE CAVITATION-INCEPTION CHARACTERISTICS OF TWO-DIMENSIONAL HYDROFOILS

Daniel T. Valentine

Naval Ship Research and Development Center

Prepared for:

Naval Ship Systems Command

July 1974

UNCLASSIFIED

SECURITY CLASSIFICATION OF THIS PAGE (When Data Entered)

REPORT DOCUMENTATION PAGE		READ INSTRUCTIONS BEFORE COMPLETING FORM
1. REPORT NUMBER: 3813	2. GOVT ACCESSION NO.	3. RECIPIENT'S CATALOG NUMBER: AD-785 834
4. TITLE (and Subtitle): THE EFFECT OF NOSE RADIUS ON THE CAVITATION-INCEPTION CHARACTERISTICS OF TWO-DIMENSIONAL HYDROFOILS		5. TYPE OF REPORT & PERIOD COVERED
		6. PERFORMING ORG. REPORT NUMBER
7. AUTHOR(s): Daniel T. Valentine		8. CONTRACT OR GRANT NUMBER(s)
9. PERFORMING ORGANIZATION NAME AND ADDRESS: Naval Ship Research and Development Center, Bethesda, Maryland 20034		10. PROGRAM ELEMENT, PROJECT, TASK AREA & WORK UNIT NUMBERS: Task 12231, Program Element 63508N, Work Unit 1-1544-005
11. CONTROLLING OFFICE NAME AND ADDRESS: Naval Ship Systems Command, Washington, D. C. 20360		12. REPORT DATE: July 1974
		13. NUMBER OF PAGES: 49
14. MONITORING AGENCY NAME & ADDRESS (if different from Controlling Office)		15. SECURITY CLASS. (of this report): UNCLASSIFIED
		15a. DECLASSIFICATION/DOWNGRADING SCHEDULE

16. DISTRIBUTION STATEMENT (of this Report)

APPROVED FOR PUBLIC RELEASE: DISTRIBUTION UNLIMITED

17. DISTRIBUTION STATEMENT (of the abstract entered in Block 20, if different from Report)

18. SUPPLEMENTARY NOTES

19. KEY WORDS (Continue on reverse side if necessary and identify by block number)

Hydrofoils
Cavitation Inception
Pressure Distribution

20. ABSTRACT (Continue on reverse side if necessary and identify by block number)

Results of an analytical investigation of the cavitation-inception characteristics of modified marine propeller-type hydrofoils are presented. In particular, dependence of the critical cavitation number and the cavitation-free, angle-of-incidence range on changes in the leading-edge thickness is determined. It is shown that within a narrow range of changes of leading-edge thickness, a delay in inception is possible, depending on the design problem under consideration. An increase in critical inception speed, accompanied by a sacrifice in some of the cavitation-free,

(Continued on reverse side)

DD FORM 1 JAN 73 1473 EDITION OF 1 NOV 65 IS OBSOLETE
S/N 0102-014-6601

UNCLASSIFIED

SECURITY CLASSIFICATION OF THIS PAGE (When Data Entered)

(Block 20 continued)

angle-of-incidence range occurs for a small increase in the leading-edge thickness. A range of thickness changes exists for which beneficial results can be obtained.

TABLE OF CONTENTS

LIST OF FIGURES

LIST OF TABLES

NOTATION

C_L	Lift coefficient $C_L = LIFT/[(1/2)\rho\ U^2\ c]$
C_N	Nose radius constant $C_N = \rho_{LE}/\tau^2$
C_P	Pressure coefficient $C_P = (p - p_\infty)/[(1/2)\rho\ U^2]$
c	Chord length
f_M	Maximum camber ratio f_M = camber/chord
N	Thickness parameter defined by Equation (1)
p	Local static pressure on section
p_V	Vapor pressure on the liquid
p_∞	Free-stream static pressure
U	Velocity of section
x	Fraction of chord, measured from leading edge
Y_T	Thickness ordinate, divided by chord length
Y_C	Camber line ordinate, divided by chord length
α	Angle of attack
ϵ_i	Thickness parameter defined by Equation (6)
ρ	Fluid mass density
ρ_{LE}	Nondimensional leading-edge radius $\rho_{LE} = C_N\ \tau^2$
σ	Cavitation number $\sigma = (p_\infty - p_V)/(1/2)\rho\ U^2$
σ_c	"Critical" cavitation number, defined in Figure 7
σ_d	Cavitation number defined in Figure 7
τ	Thickness ratio, twice maximum thickness ordinate
ψ	Relative divergence of inception curve, defined in Figure 7

ABSTRACT

Results of an analytical investigation of the cavitation-inception characteristics of modified marine propeller-type hydrofoils are presented. In particular, dependence of the critical cavitation number and the cavitation-free, angle-of-incidence range on changes in the leading-edge thickness is determined. It is shown that within a narrow range of changes of leading-edge thickness, a delay in inception is possible, depending on the design problem under consideration. An increase in critical inception speed, accompanied by a sacrifice in some of the cavitation-free, angle-of-incidence range occurs for a small increase in the leading-edge thickness. A range of thickness changes exists for which beneficial results can be obtained.

ADMINISTRATIVE INFORMATION

The project was authorized and funded by the Naval Ship Systems Command under Task, 12231 and Program Element 63508N; Work Unit 1-1544-005.

INTRODUCTION

PROBLEM

Prediction of cavitation inception on propeller blades, struts, appendages and other ship and submarine control surfaces is important since even small amounts of cavitation can lead to erosion and noise problems. Knowledge of the cavitation-inception characteristics of two-dimensional hydrofoil sections is useful in choosing the appropriate section for a particular design application.[1,2] In this report modifications of the hydrofoil sections used in the design of modern marine propellers are investigated theoretically, albeit the results are applicable to any hydrofoil design problem.

The investigation was undertaken with the objective of determining the effect of increasing the leading-edge thickness on cavitation performance of marine propellers. Impetus for the investigation was the necessity to sometimes change the leading- and/or trailing-edge thicknesses in order to satisfy various design requirements. An increase in thickness at the trailing edge may be required by strength considerations. An increase in thickness at the

---

[1] Brockett, T., "Steady Two-Dimensional Pressure Distributions on Arbitrary Profiles," David Taylor Model Basin Report 1821 (1965). A complete listing of references is given on pages 40 and 41.

[2] Brockett, T., "Minimum Pressure Envelopes for Modified NACA-66 Sections with NACA a = 0.8 Camber and BUSHIPS Type I and II Sections," David Taylor Model Basin Report 1780 (1966).

leading edge may be required to provide space for air ducts in the propeller blade in the vicinity of the leading edge. Assessment of these design modifications on the cavitation-inception characteristics of the hydrofoils is needed and, consequently, is the purpose of the investigation.

The approach taken in investigating the change in hydrofoil leading-edge shape was to determine the effect on the cavitation-inception characteristics of varying the nose radius by varying the leading-edge thickness of propeller-type hydrofoils. A transformation was used to vary the leading-edge thickness so that no change would occur either in the position of the leading edge and midchord or in the maximum thickness of the modified hydrofoils. In addition, the effect was determined of a typical foil-modification method used by the Naval Ship Engineering Center on the cavitation-inception characteristics of the hydrofoils used in a recent propeller design. Both modification methods are described in detail in the appropriate sections of this report, as well as a comparison of their cavitation-inception characteristics.

The results presented in this report concern the effect of the leading edge or nose radius on the cavitation-inception characteristics of the parent NACA 66 (TMB modified) and BUSHIPS Hydrofoils. These hydrofoils were chosen because of their use in the design of marine propellers. Results are presented on the effect of nose thickening on the cavitation-inception characteristics of symmetric and cambered hydrofoils. A comparison of the parent and modified hydrofoils is given. The effect of the leading-edge shape as an independent foil parameter such as thickness, camber, and chord is discussed. Such knowledge is useful in design problems where the given design constraints restrict the choice of the foil shape so that the parent foils are inadequate. In this case, if only small modifications are necessary, the procedure and results presented should prove useful.

LITERATURE REVIEW

The cavitation-inception characteristics of the hydrofoils investigated have been reported by Eckhardt and Morgan,[3] Milam and Morgan,[4] Caster,[5] and Brockett.[2] Brockett[2] showed that the NACA 66 (TMB modified) thickness form and an a = 0.8 mean line exhibited very nearly the same cavitation-inception characteristics in comparison to the BUSHIPS type sections (NACA 16 thickness form and NACA 65 parabolic mean line). For most propeller-design problems both sections can be considered good from the point of view of propeller-blade cavitation.

---

[3]Eckhardt, M. K. and W. B. Morgan, "A Propeller Design Method," Society of Naval Architects and Marine Engineers Transactions, Vol. 63, pp. 325–374 (1955).

[4]Milam, A. and W. B. Morgan, "Section Moduli and Incipient Cavitation Diagrams for a Number of NACA Sections," David Taylor Model Basin Report 1177 (1957).

[5]Caster, E., "Incipient Cavitation Diagrams for BUSHIPS Type I and II Sections," David Taylor Model Basin Report 1643 (1962).

For the propeller-design problem, Morgan and Lichtman[6] illustrated the usefulness of the cavitation-inception characteristics as presented by Brockett.[2] Figures 1 through 6 are examples taken from the Brockett report of the cavitation-inception curves which apply to the parent hydrofoils considered in this report. The curves show the effect of incidence angle on the minimum pressure coefficient for a particular hydrofoil section. The curves are plotted for different thickness and camber ratios, illustrating the effect of thickness and camber on cavitation-inception characteristics. As the thickness ratio increases, the cavitation-inception speed at the shock-free incidence angle decreases, and the cavitation-free angle of attack range increases. The effect of increasing camber for a constant thickness-to-chord ratio is to decrease the shock-free, attack angle inception speed and to increase the fluctuation range of cavitation-free angle of attack.

Mandel[7] in 1953 plotted the minimum pressure coefficient versus the nose radius for 58 NACA symmetrical airfoil sections for several attack angles. This composite plot showed that for a given attack angle there existed an optimum nose radius, i.e., a nose radius at which the minimum pressure versus nose radius curve exhibited a maximum. Optimum nose radius increased with increasing attack angle.

Alef[8] studied analytically, relatively sharp-nosed ($0.36 < \rho_{LE}/\tau^2 < 0.72$) symmetrical airfoil shapes at small attack angles of less than 6 degrees. The term ρ_{LE}/τ^2 equal to 0.5 corresponds to an elliptical nose shape for the polynomial defined foils investigated by Alef. For "great values" of the nose radius (ρ_{LE}/τ^2 near 0.72) Alef found that a suction peak occurred near the leading edge. As the nose radius decreased this suction peak decreased. Also, the chordwise extent of the suction decreased with decreasing nose radius. Looking at a hypothetical inception curve (Figure 7) Alef found that the relative divergence of the cavitation inception diagram increased with increasing nose radius while the design-point angle of attack variation δ decreased.

Breslin and Landweber[9] reviewed the cavitation inception literature to 1961. They presented results which showed that for a series of foil shapes at zero angle of attack with a nose thickness parameter, the ratio of the nondimensional nose radius to the thickness ratio

---

[6]Morgan, W. B. and J. P. Lichtman, "Cavitation Effects on Marine Devices," Cavitation State of Knowledge published by American Society of Mechanical Engineers (Jun 1969).

[7]Mandel, P., "Some Hydrodynamic Aspects of Appendage Design," Society of Naval Architects and Marine Engineers Transactions, Vol. 61, pp. 464–515 (1953).

[8]Alef, W. E., "Propeller Sections to be Used in a Non-Homogeneous Wake," Hamburg Model Basin Report 1187 (Jun 1959).

[9]Breslin, J. P. and L. Landweber, "A Manual for Calculation of Inception of Cavitation on Two and Three Dimensional Forms," Society of Naval Architects and Marine Engineers T & R Bulletin 1-21 (Oct 1961).

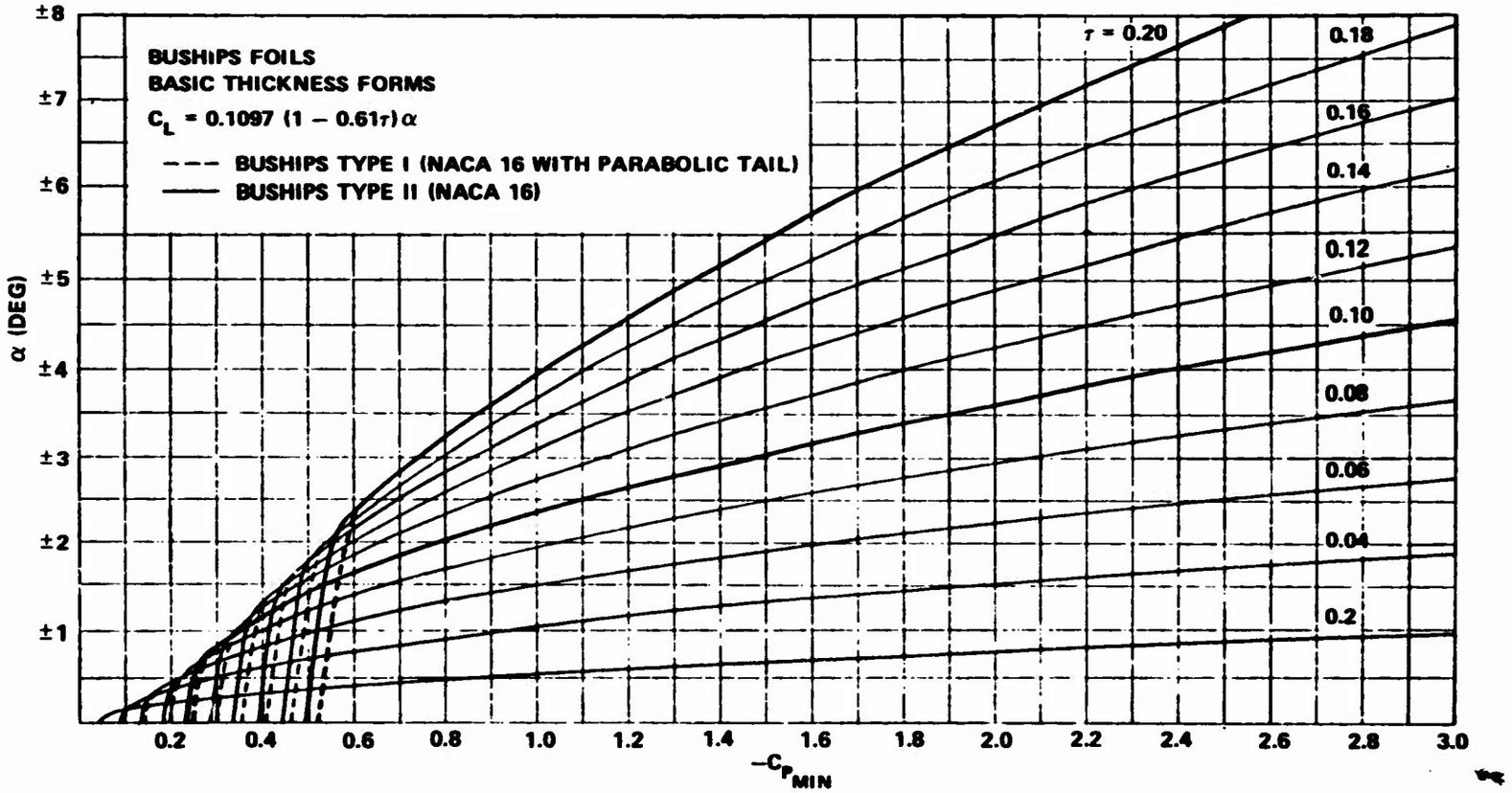

Figure 1 – Minimum Pressure Envelopes for BUSHIPS Type I and Type II Sections with Zero Camber

(Taken from Reference 2)

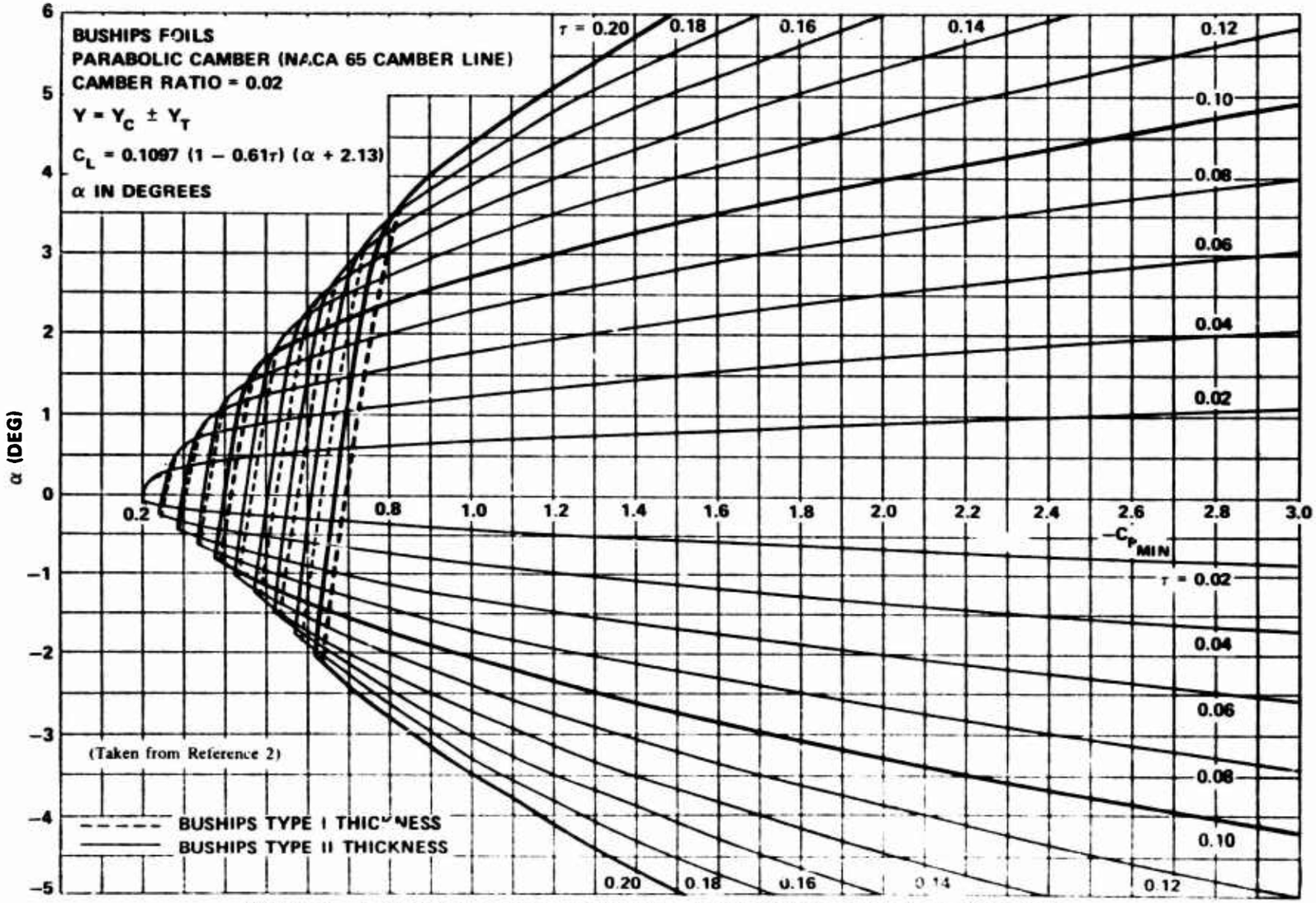

Figure 2 – Minimum Pressure Envelopes for BUSHIPS Type I and Type II Sections Having a Maximum Camber Ratio of 0.02

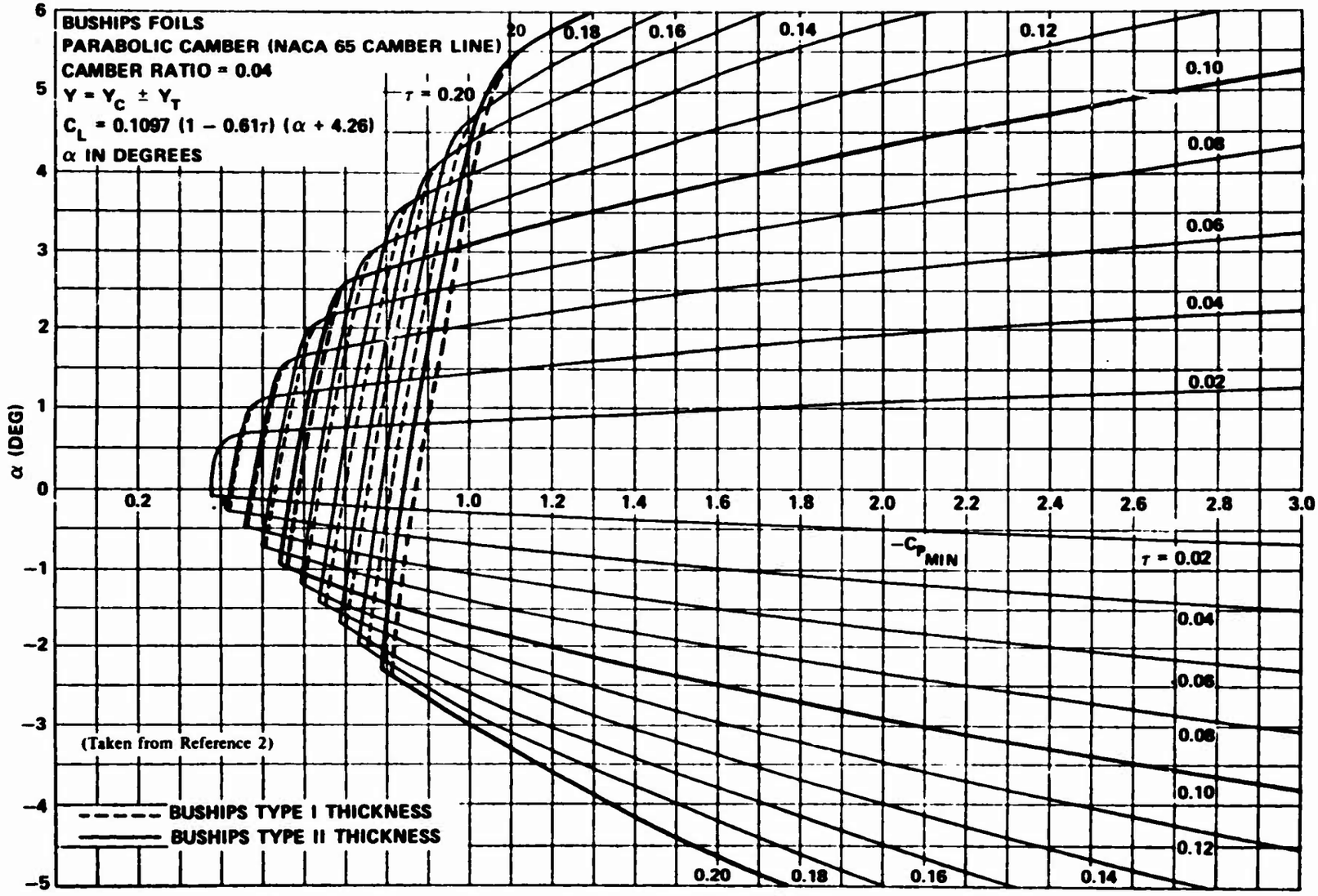

Figure 3 – Minimum Pressure Envelopes for BUSHIPS Type I and Type II Sections Having a Maximum Camber Ratio of 0.04

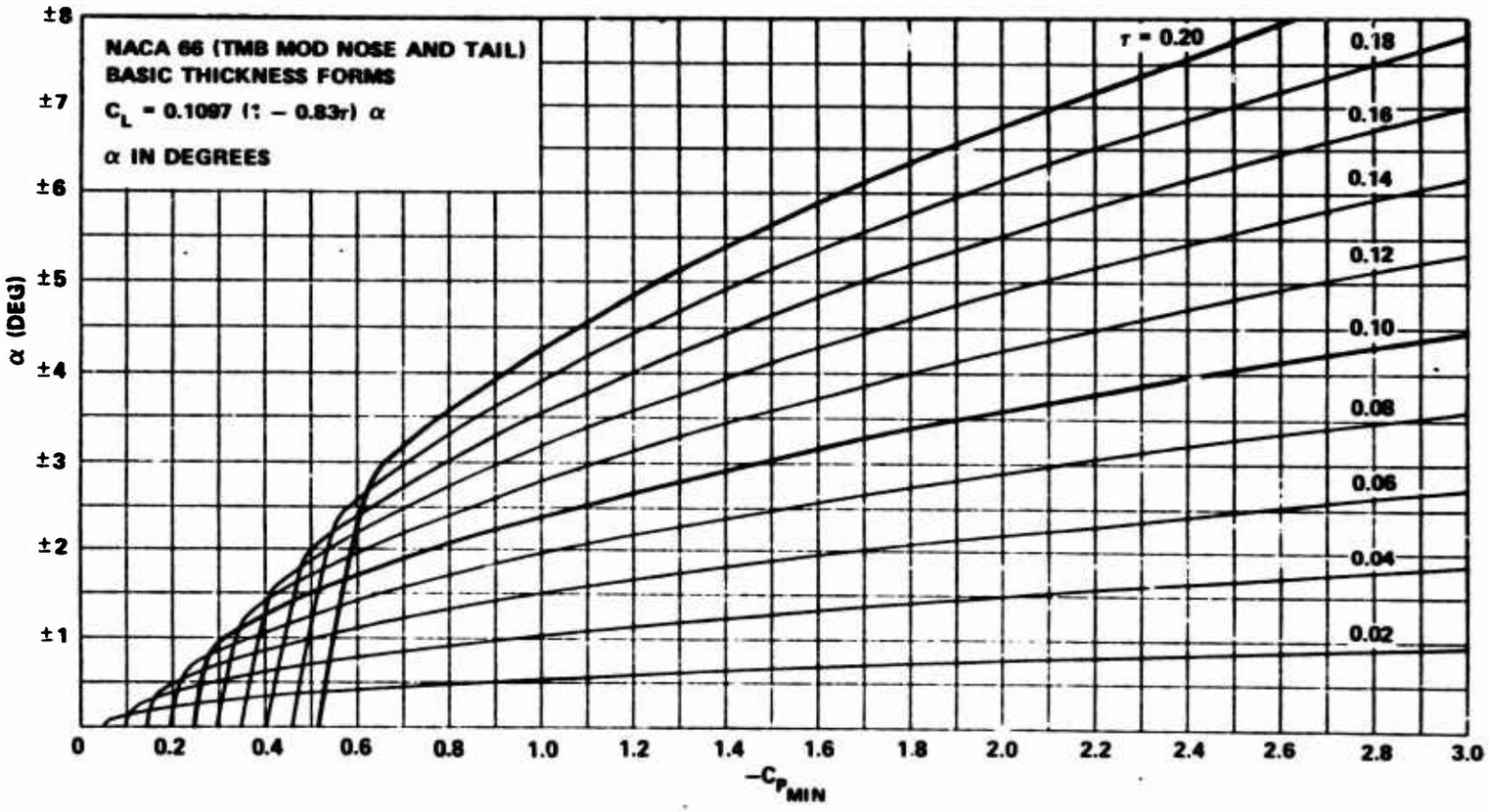

Figure 4 – Minimum Pressure Envelopes for NACA 66 (TMB Modified) Sections with Zero Camber

(Taken from Reference 2)

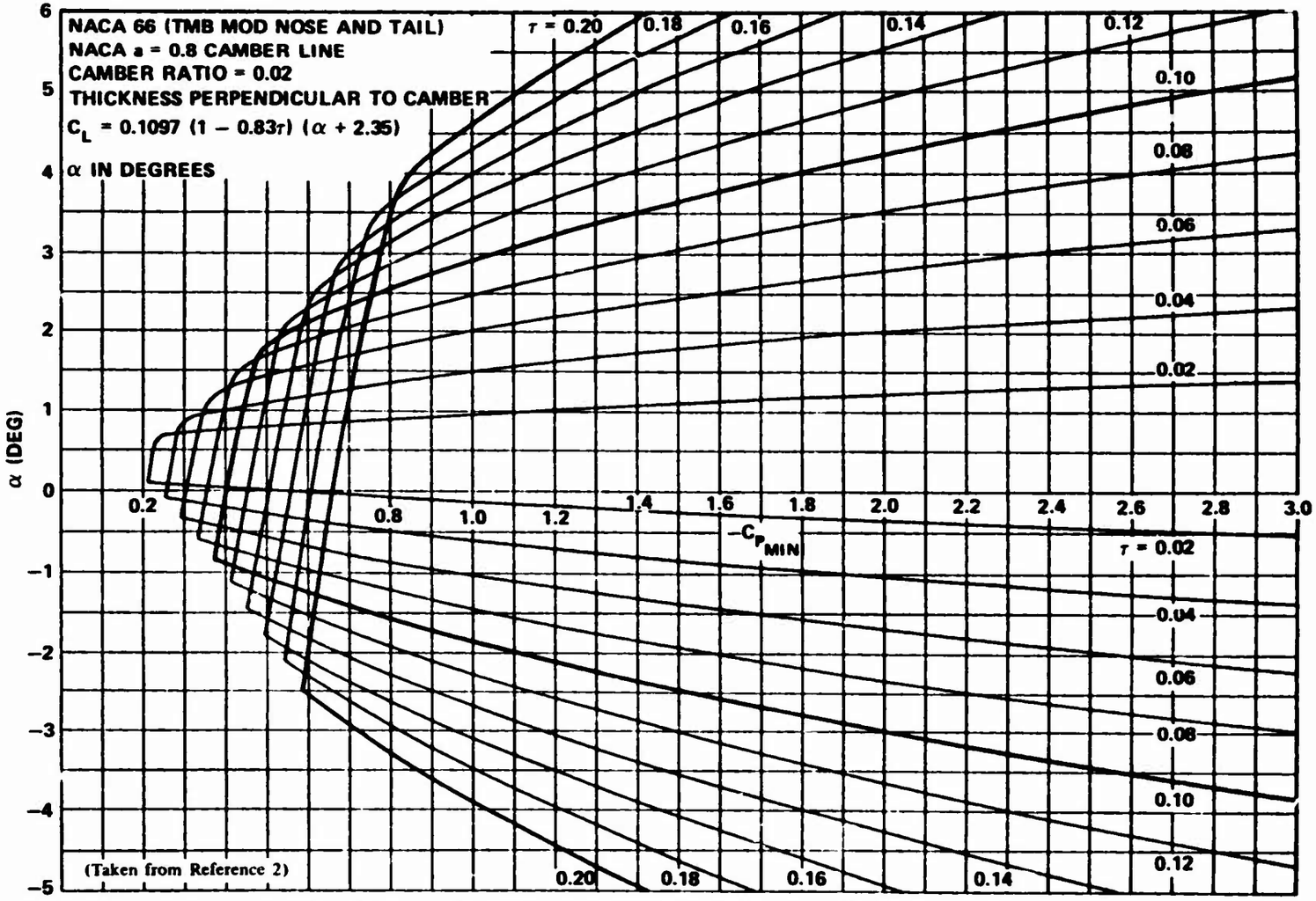

Figure 5 – Minimum Pressure Envelopes for NACA 66 (TMB Modified) Sections Having a Maximum Camber Ratio of 0.02

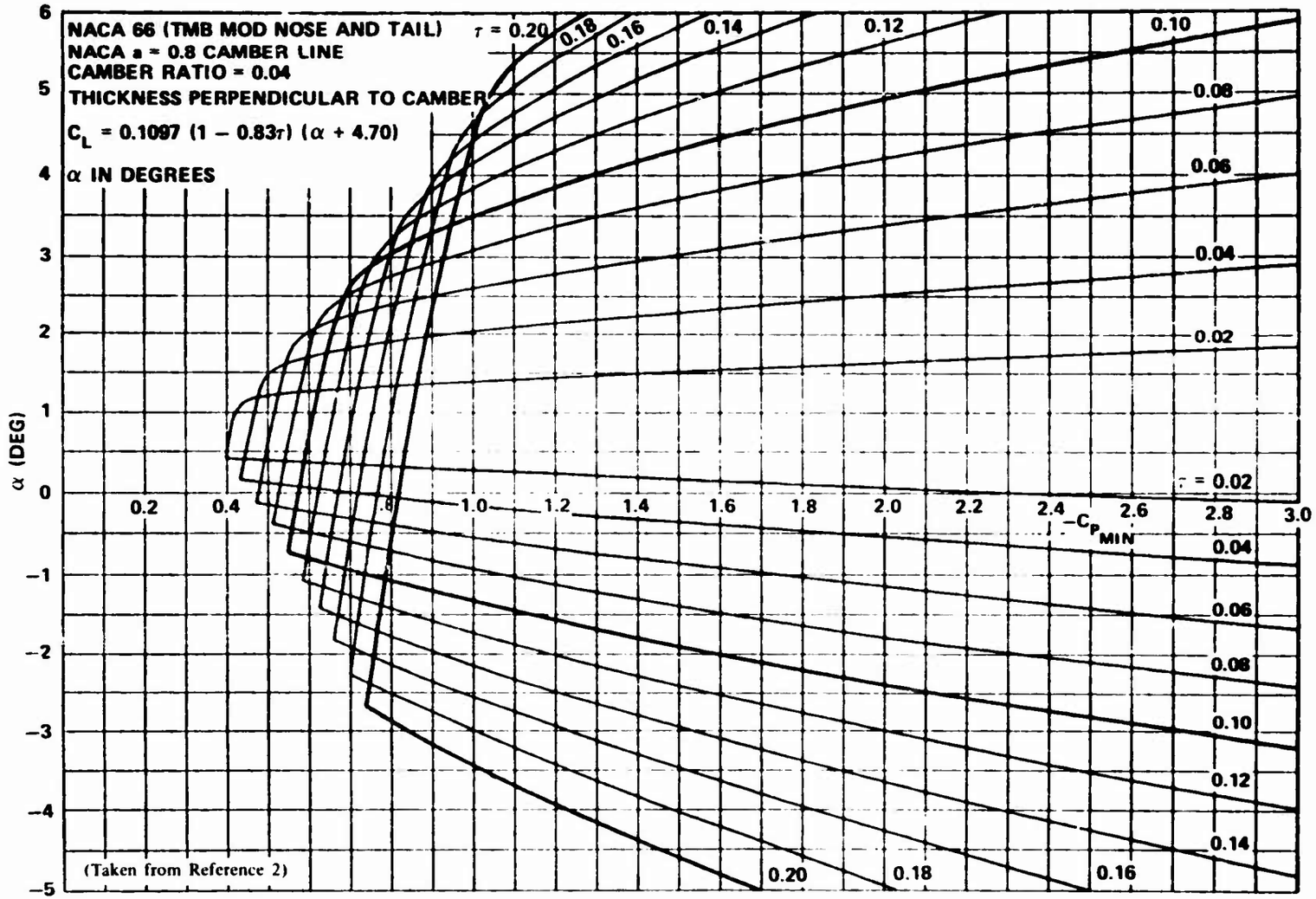

Figure 6 - Minimum Pressure Envelopes for NACA 66 (TMB Modified) Sections Having a Maximum Camber Ratio of 0.04

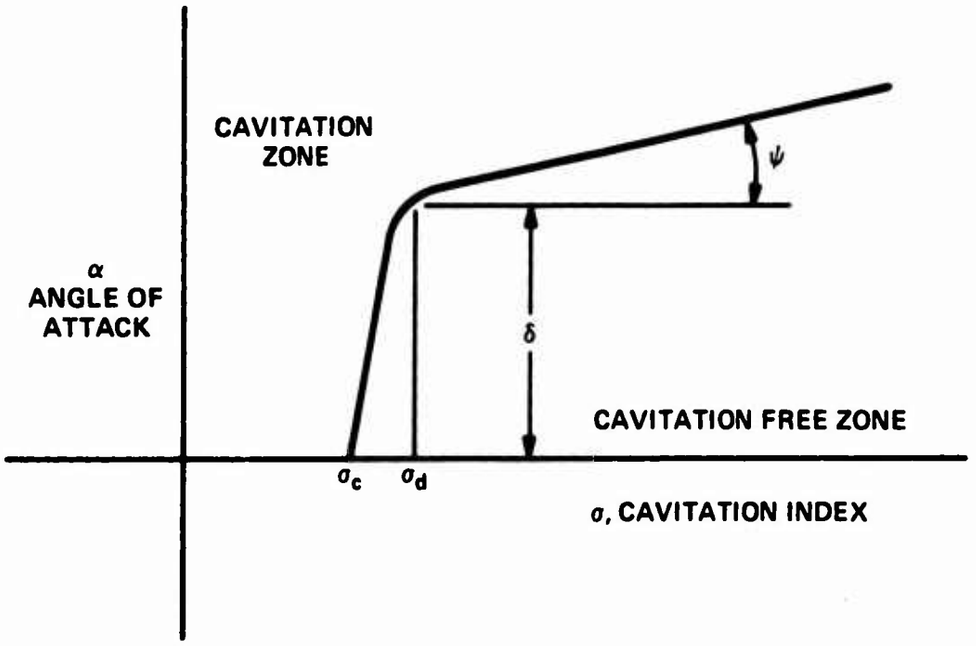

Figure 7 – Minimum Pressure Envelope for a Propeller-Type Basic Thickness Form

squared (ρ_{LE}/τ^2), slightly greater than 0.5 exhibited the smallest suction peak. Therefore, one conclusion is that, if choosing a foil to operate at or near its shock-free entry angle of attack, the foil should be nearly elliptical with a nose radius parameter, ranging from 0.5 to 0.8; see Figure 8, taken from Reference 9. The data leading to this conclusion was first presented by Berggren and Graham.[10]

Spurred by the work of Mandel[7] and Alef,[8] Collins and Evans[11] investigated the effects of several foil parameters on the cavitation characteristics of several foil shapes at large angles of attack, i.e., greater than 6 degrees. The foils considered were the polynomial shapes developed by Alef. All the cases considered were for symmetric shapes. Confirmation of the existence of an optimum nose radius for each angle of attack was found.

The optimum nose radius for a given attack angle depends on the position of maximum thickness and is effectively independent of thickness-to-chord ratio and other section parameters. For practical considerations, it is well to note that the minimum pressure coefficient, or critical cavitation index, does not appreciably vary in the region of the optimum nose radius.

The fact that an increase in the leading-edge radius may increase the resistance to cavitation near the design cavitation index was also found by Moeckel in 1966.[12] By increasing the leading-edge radius of a NACA 16-X08 cambered foil, X = 0.390, Moeckel calculated a reduction in the inception velocity in the attack angle range of -2 degrees $< \alpha < +1$ degree. Beyond this range of attack angles, an increase in the inception velocity was calculated.

The present investigation is an extension of the work of Brockett, Evans and Collins, Alef, and Breslin and Landweber, which is to investigate the effect of changes in leading-edge thickness on the cavitation-inception characteristics of symmetric and cambered marine-propeller-type hydrofoils not reported before.

INVESTIGATION PROCEDURE

HYDROFOIL SECTIONS

The NACA 66 (TMB modified) and BUSHIPS Type II hydrofoil sections were chosen for this investigation because of their use in the design of marine propellers. The NACA 66

---

[10] Berggren, R. E. and D. J. Graham, "Effects of Leading Edge Radius and Maximum Thickness-Chord Ratio on the Variation with Mach Number of the Aerodynamic Characteristics of Several NACA Airfoil Sections," National Advisory Committee for Aeronautics TN 3172 (1954).

[11] Collins, I. F. and A. M. Evans, "Theoretical Study of the Cavitation Resistance of Aerofoil Sections at Incidence," Admiralty Research Laboratory Report ARL/R4/G/AE/2/5 (Nov 1965).

[12] Moeckel, G. P., "The Effect of Distortion of Subcavitating Foil Contours on Cavitation-Inception Velocity," Journal of Ship Research, pp. 253–262 (Dec 1966).

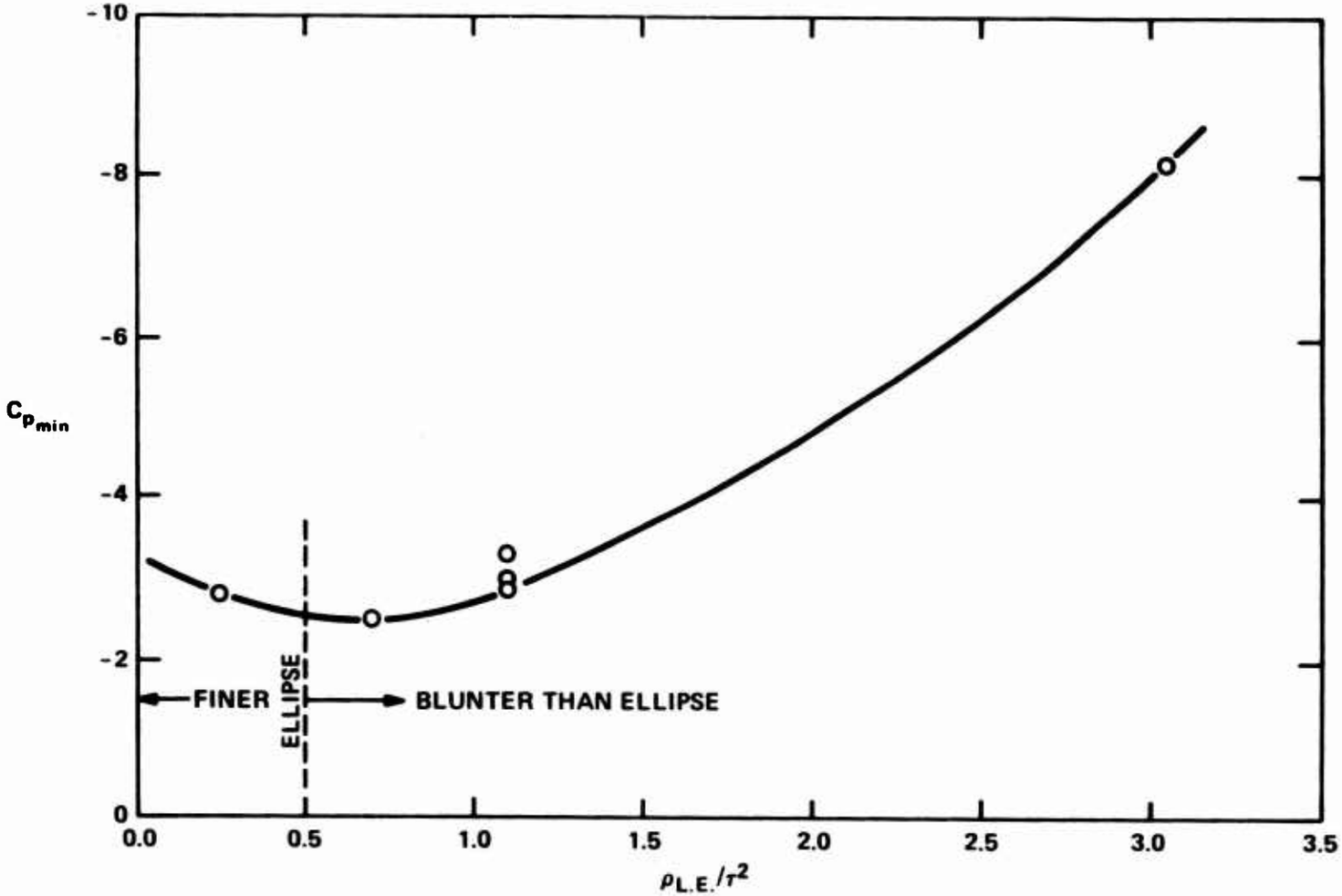

Figure 8 - Influence of Nose Radius on the Minimum Pressure Coefficient for NACA 4-Digit Foils at Zero Angle of Attack

(Taken from Reference 9; see 10, also)

(TMB modified) section is the hydrofoil section first given by Eckhardt and Morgan[3] and modified by Brockett[2] to obtain a smooth, flat, pressure-distribution curve, based on the program Brockett developed. Using these sections as the starting point, the modifications consisted of effectively changing the leading-edge radius.

The leading-edge radius was varied by shifting the contour of the thickness form in the y-direction from the leading edge to the point of maximum thickness. The transformation equation used is

$$(Y_T/\tau)_N = (1/2)[2(Y_T/\tau)_{1.0}]^{1/N} \qquad (1)$$

where $(Y_T/\tau)_{1.0}$ = thickness-form offsets of parent foil section being considered

$(Y_T/\tau)_N$ = modified thickness-form offsets from leading edge to point of maximum thickness

This method of modification was chosen to ensure that no change in the foil-section chord length and maximum thickness occurred. Values of N greater than unity correspond to leading-edge radii greater than the radius of the parent section. The parent thickness-form offsets, the camber-line offsets, and the modified thickness-form offsets for the modified leading-edge radius sections are given in Tables 1 and 2 for the NACA 66 (TMB modified) and BUSHIPS type sections, respectively.

For the given foil shapes, the leading-edge radius is proportional to the maximum thickness squared, i.e.

$$\rho_{LE} = C_N \tau^2 = \text{leading-edge radius/chord length} \qquad (2)$$

The constant C_N depends on the thickness distribution, or foil geometry, in the vicinity of the leading edge. The nose radius can be found from the change in slope near the leading edge, which is given in the computer output of the symmetric foil.[1] The constants for the modified foils are given in Table 3.

CAVITATION-INCEPTION CHARACTERISTICS

The pressure distribution at various angles of attack was calculated, using the two-dimensional, pressure-distribution program developed at the Center.[1] The method used was an arbitrary conformal mapping approach with viscous corrections. The method required the lift curve slope η and the zero lift angle of attack α_{oe}. These experimentally determined parameters yielded the lift coefficient as follows

TABLE 1 – N-MODIFIED FOIL GEOMETRIES OF NACA 66 (TMB MODIFIED) AT CONVENTIONAL STATIONS

Station	Thickness Ordinate $(Y_T/\tau)_N$ for N Equal							NACA a = 0.8 Camber Line	
x	1.3	1.1	1.05	1.0	0.95	0.9	0.8	Camber Ordinate Y_C/f	Camber Slope $(dY_C/dx)/f$
0	0	0	0	0	0	0	0	0	–
0.005	0.10593	0.07989	0.07321	0.0665	0.05980	0.05315	0.04016	0.0423	7.149
0.0075	0.12352	0.09579	0.08854	0.0812	0.07379	0.06635	0.05155	0.0595	6.617
0.0125	0.14986	0.12038	0.11249	0.1044	0.09614	0.08772	0.07057	0.0907	5.944
0.025	0.19458	0.16390	0.15542	0.1466	0.13743	0.12792	0.10788	0.1586	5.023
0.05	0.25334	0.22389	0.21548	0.2066	0.19721	0.18728	0.16564	0.2712	4.083
0.075	0.29562	0.26868	0.26085	0.2525	0.24358	0.23404	0.21285	0.3657	3.515
0.1	0.32946	0.30539	0.29831	0.2907	0.28252	0.27370	0.25384	0.4482	3.100
0.15	0.38178	0.36351	0.35803	0.3521	0.34566	0.33864	0.32254	0.5869	2.488
0.2	0.42114	0.40820	0.40427	0.4000	0.39533	0.39020	0.37830	0.6993	2.023
0.25	0.45024	0.44174	0.43914	0.4363	0.43318	0.42974	0.42974	0.7905	1.635
0.3	0.47184	0.46689	0.46537	0.4637	0.46186	0.45983	0.45504	0.8635	1.292
0.35	0.48703	0.48470	0.48399	0.4832	0.48233	0.48127	0.47909	0.9202	0.933
0.4	0.49630	0.49563	0.49543	0.4952	0.49495	0.49467	0.49401	0.9615	0.678
0.45	0.50	0.50	0.50	0.5000	0.50	0.50	0.50	0.9881	0.385
0.5				0.4962				1.0	0.091
0.55				0.4846				0.9971	–0.211
0.6				0.4653				0.9786	–0.532
0.65				0.4383				0.9434	–0.885
0.7				0.4035				0.8892	–1.295
0.75				0.3612				0.8121	–1.813
0.8				0.3110				0.7027	–2.712
0.85				0.2532				0.5425	–3.523
0.9				0.1877				0.3586	–3.768
0.95				0.1143				0.1713	–3.668
0.975				0.0748				0.0823	–3.441
1.0				0.0333				0.0	–3.003

NOTE. Only the leading portion of the thickness form is varied. The trailing edge for all the foils is the same as N = 1.0.

TABLE 2 – N-MODIFIED BUSHIPS FOIL GEOMETRIES AT CONVENTIONAL STATIONS

Station x	Type II Thickness			Type I Thickness		NACA 65 Mean Line Ordinate
	N = 1.1 $(Y_T/\tau)_{1.1}$	N = 1.05 $(Y_T/\tau)_{1.05}$	N = 1.0 $(Y_T/\tau)_{1.0}$	N = 1.0 $(Y_T/\tau)_{1.0}$	$\epsilon_1/c\tau$ = 0.05277 $(Y_T/\tau)_{\epsilon_1}$	Y_C/f
0	0	0	0	0	0	0
0.005	0.08232	0.07554	0.06873	0.06873	0.11425	0.0199
0.0075	0.09864	0.09130	0.08386	0.08386	0.12778	0.029775
0.0125	0.12371	0.11575	0.10758	0.10758	0.14900	0.049375
0.025	0.16775	0.15924	0.15039	0.15039	0.18729	0.0975
0.05	0.22633	0.21794	0.20908	0.20908	0.23978	0.19
0.075	0.26872	0.26089	0.25254	0.25254	0.27866	0.2775
0.1	0.30281	0.29577	0.28800	0.28800	0.31037	0.36
0.15	0.35641	0.35071	0.34455	0.34455	0.36096	0.51
0.2	0.39760	0.39328	0.38859	0.38859	0.40035	0.64
0.25	0.43013	0.42705	0.42370	0.42370	0.43175	0.75
0.3	0.45566	0.45365	0.45145	0.45145	0.45657	0.84
0.35	0.47516	0.47401	0.47275	0.47275	0.47563	0.91
0.4	0.48895	0.48853	0.48786	0.48786	0.48914	0.96
0.45	0.49723	0.49709	0.49695	0.49695	0.49727	0.99
0.5	0.5	0.5	0.5	0.5	0.5	1.0
0.55			0.49674	0.495	0.49625	0.99
0.6			0.48624	0.48	0.48502	0.96
0.65			0.46740	0.455	0.46629	0.91
0.7			0.43912	0.42	0.44008	0.84
0.75			0.40031	0.375	0.40637	0.75
0.8			0.34988	0.32	0.36518	0.64
0.85			0.28673	0.255	0.31649	0.51
0.9			0.20976	0.18	0.26023	0.36
0.95			0.11788	0.095	0.1620	0.19
0.975			0.06601	0.04875	0.0890	0.0975
1.0			0.01	0.0	0.0	0

NOTE: For N-thickness forms only the leading portion is varied; trailing edge for all foils is the same as for N = 1.0.

TABLE 3 – LEADING-EDGE RADII FOR NACA 66 (TMB MODIFIED) AND BUSHIPS TYPE II N- AND ϵ MODIFIED HYDROFOILS

Hydrofoil	N	$\epsilon_1/c\tau^*$	C_N
NACA 66 (TMB modified)	1.3	–	1.272
	1.1	–	0.674
	1.05	–	0.556
	1.0	–	0.448
	0.95	–	0.355
	0.9	–	0.272
NACA 66 (TMB modified)	0.8	–	0.144
BUSHIPS II	1.1	–	0.751
BUSHIPS II	1.05	–	0.607
BUSHIPS II and I	1.0	–	0.48889
BUSHIPS I	–	0.05277*	1.459
$\rho_{LE} = C_N \tau^2$ = LEADING-EDGE RADIUS/CHORD LENGTH			

*Refer to Equation (6) in text.

$$C_L = 2\pi\eta(\alpha - \alpha_{oe}) \tag{3}$$

For high Reynolds number, α_{oe} and η are independent and can be determined by the following approximate formulas,[2] i.e., the lift coefficient for NACA 66 (TMB modified) sections with an NACA a = 0.8 camber line becomes

$$C_L = 2\pi(1 - 0.83\tau)(\alpha + 2.05f) \tag{4}$$

For the BUSHIPS section

$$C_L = 2\pi(1 - 0.61\tau)(\alpha + 1.86f) \tag{5}$$

For the modified section shapes the experimental lift data are not available; therefore, the assumption has been made that α_{oe} and η values do not change significantly with small modifications in the thickness distribution. Pinkerton[13] found experimentally that the slope of the lift curve and the zero lift angles of attack were independent of small changes in the leading-edge radius and of small changes in the thickness distribution.

From the pressure distribution at a given attack angle, the minimum pressure is determined. Cavitation characteristics are shown as a plot of the attack angle α versus the minimum pressure coefficient $-C_{p_{min}}$. The cavitation criterion assumed is that the inception of cavitation occurs when the minimum pressure coefficient corresponds to the vapor pressure of the fluid in which the foil shape is moving.

RESULTS

The pressure distributions for the two parent foils are relatively flat; see Figure 9. Increasing the leading-edge radius while keeping the maximum thickness τ and the chord length c constant results in the development of a suction peak in the vicinity of the leading edge. In this case the suction peak at approximately midchord decreases. The optimum, shock-free incidence, airfoil shape would be the shape with equal suction near the leading edge and midchord at the ideal angle of attack. However, this would lead to a cavitation-inception characteristic with a cavitation-free angle of attack variation of zero at the cavitation index σ_d; see Figure 7. Whether or not this is desirable depends on the design problem.

---

[13] Pinkerton, R. M., "Effects of Nose Shape on the Characteristics of Symmetrical Airfoils," National Advisory Committee for Aeronautics TN 386 (August 1931).

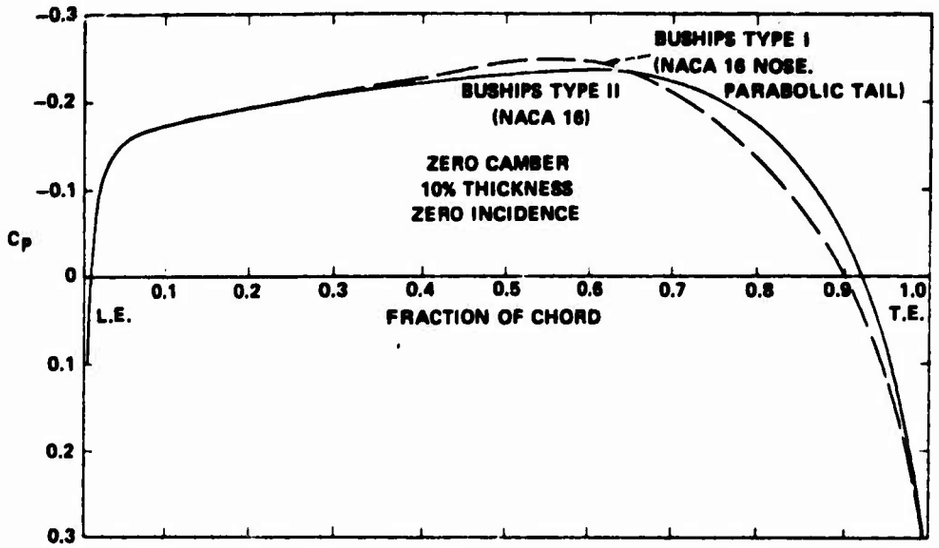

Figure 9a – Theoretical Pressure Distribution at $\alpha = 0$ Degree on BUSHIPS Foils of 10-Percent Thickness and Zero Camber

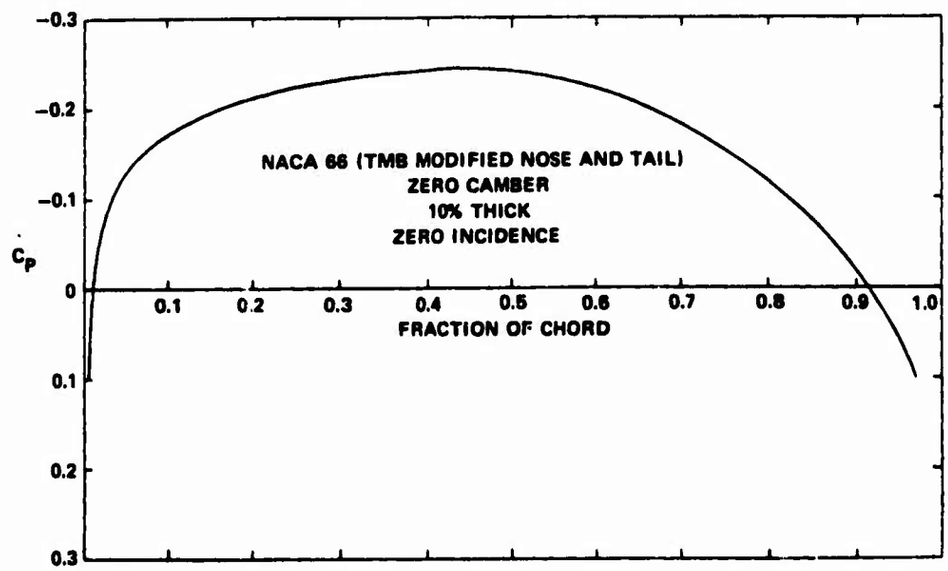

Figure 9b – Theoretical Pressure Distribution at $\alpha = 0$ Degree on the NACA 66-010 (TMB Modified Nose and Tail)

Figure 9 – Pressure Distribution on NACA 66 (TMB Modified) and BUSHIPS Type II Thickness Forms

(Taken from Reference 2)

Decreasing the leading-edge radius leads to the opposite effect, viz., the midchord suction increases while the leading-edge suction decreases. These results as well as the following results of the nose radius effects on the cavitation-inception characteristics assumes small changes in the leading-edge shape.

Figures 10 through 18 present the cavitation-inception characteristics of the modified hydrofoils as listed.

Figure	N	f_M	τ	Comment
10	1.05	0.0	Varied	N-Modified, BUSHIPS Type Hydrofoil
11	1.1	0.0	Varied	N-Modified, BUSHIPS Type Hydrofoil
12	1.1	0.02	Varied	N-Modified, BUSHIPS Type Hydrofoil
13	1.1	0.04	Varied	N-Modified, BUSHIPS Type Hydrofoil
14	1.1	0.00	Varied	N-Modified, NACA 66 (TMB modified) Hydrofoil
15	1.3	0.00	Varied	N-Modified, NACA 66 (TMB modified) Hydrofoil
16	Varied	0.00	0.23	N-Modified, NACA 66 (TMB modified) Hydrofoil
17	Varied	0.00	0.23	N-Modified, NACA 66 (TMB modified) Hydrofoil
18	Varied	0.18	0.23	N-Modified, NACA 66 (TMB modified) Hydrofoil

Figures 10 through 15 show that within the range of leading-edge variations considered, the inception characteristics are similar in shape, although the width of the cavitation-free region changes; the changes will be discussed later. Figures 16 through 18 illustrate the effect of nose radius change on the cavitation-inception curve for a fixed thickness and camber.

The NACA 66 (TMB modified) and BUSHIPS hydrofoils in use today are finer than an ellipse at the leading edge, i.e., C_N equals 0.448 and 0.489, respectively, as compared to 0.5 for ellipse. Therefore, increasing the nose radius should improve the critical, shock-free, inception speed. However, as shown in Figure 8 and in Figure 15 as compared to Figure 4, there is a limit to the increase in bluntness which will give an improved critical inception speed. From the data presented in this report, this limit is reached between an N of 1.1 and 1.3 for the propeller hydrofoils considered, which corresponds to (ρ_{LE}/τ^2) of the order of 0.7. This is consistent with the results of Berggren and Graham[10] as shown in Figure 8.

The increase in critical inception speed is obtained at the sacrifice of cavitation-free, angle-of-incidence range as shown in Figures 16 through 18. On the other hand, decreasing the nose radius is shown to increase the cavitation-free incidence range with a small sacrifice in the critical inception cavitation index. This beneficial effect of decreasing nose radius has also been found to have a limit. For the propeller-type hydrofoils a range of N exists in which benefits of either critical shock free inception speed, or increase in cavitation-free,

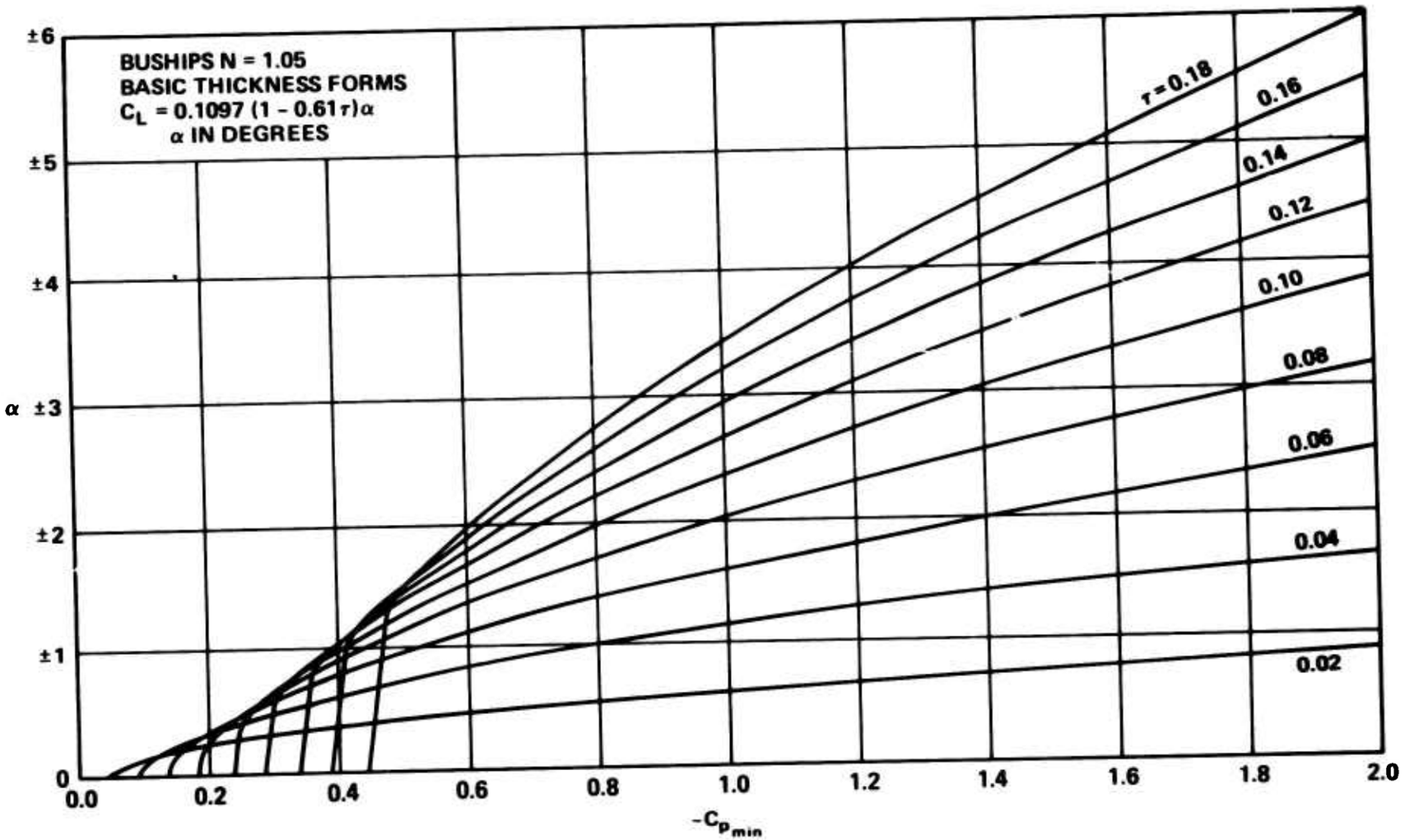

Figure 10 – Minimum Pressure Envelopes for BUSHIPS Type II, N = 1.05 Sections with Zero Camber

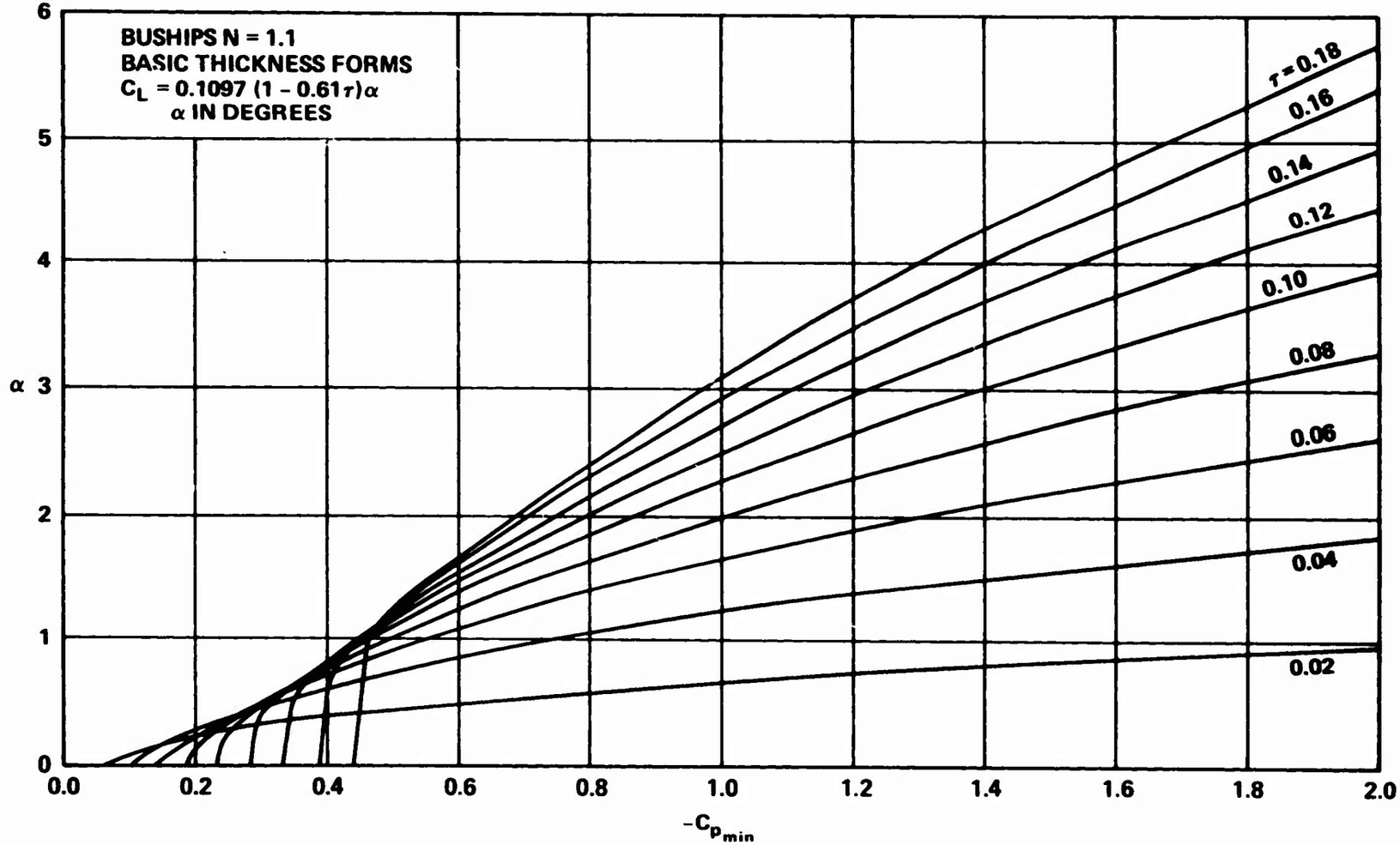

Figure 11 – Minimum Pressure Envelopes for BUSHIPS Type II, N = 1.1 Sections with Zero Camber

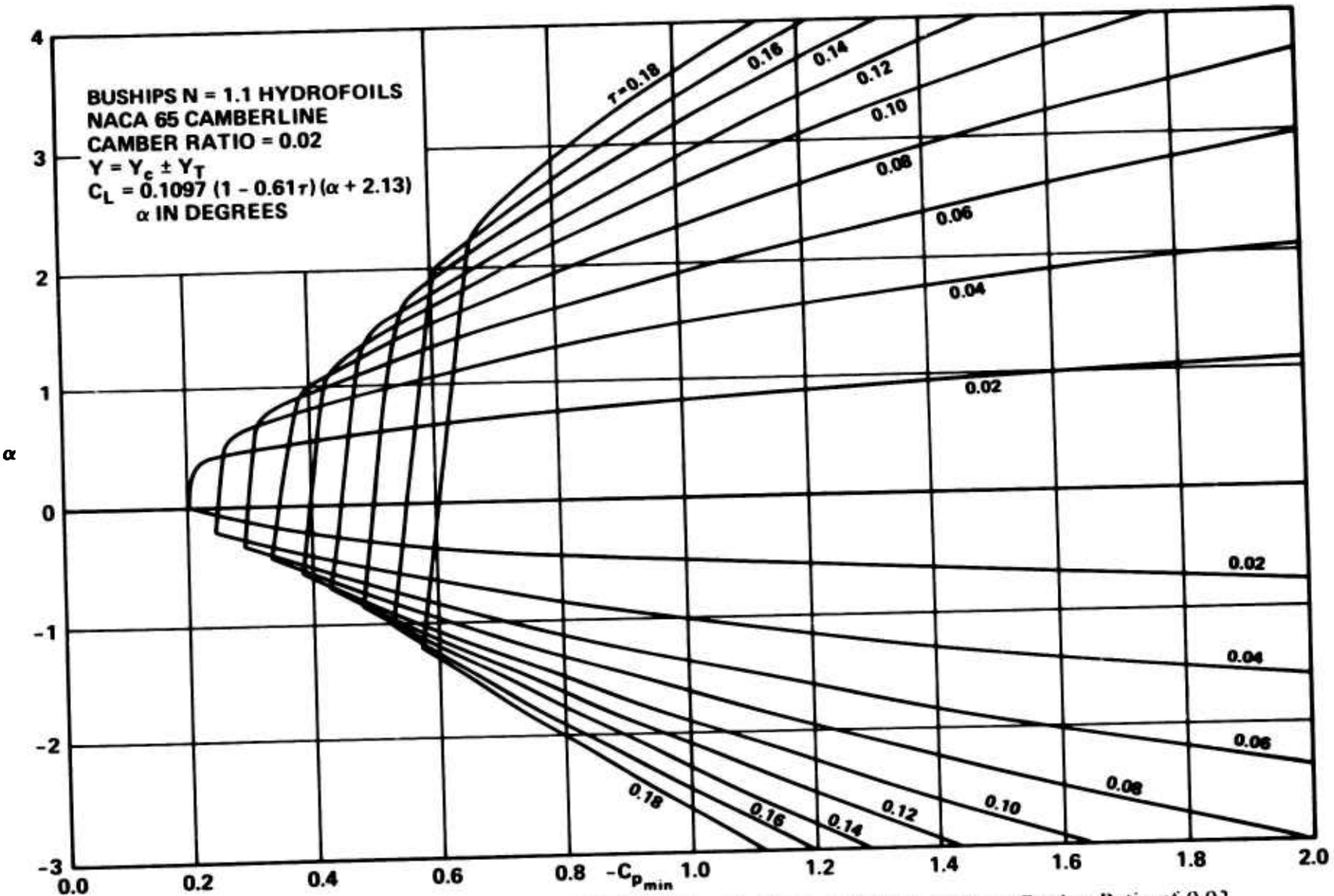

Figure 12 – Minimum Pressure Envelopes for BUSHIPS Type II, N = 1.1 Sections Having a Camber Ratio of 0.02

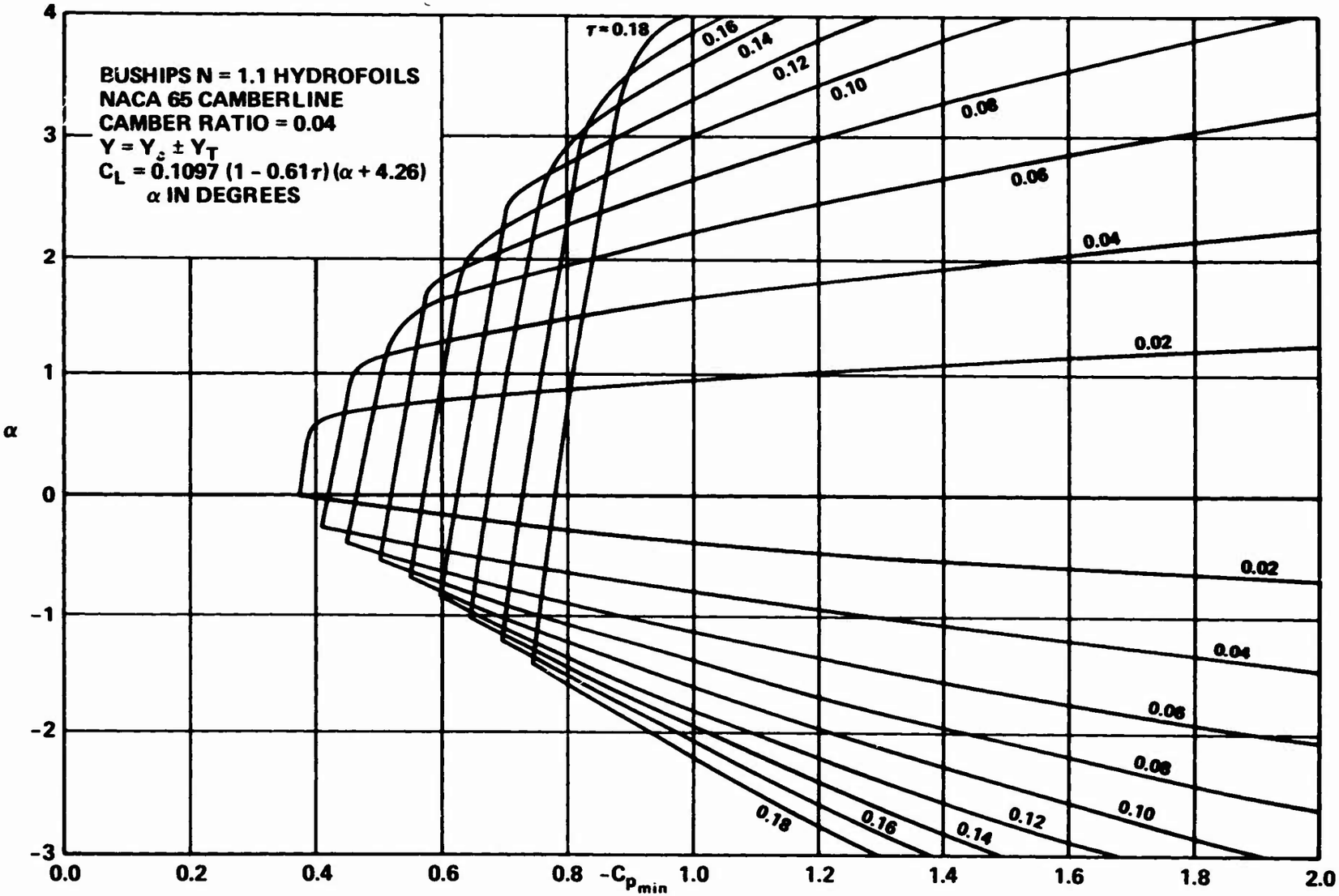

Figure 13 -- Minimum Pressure Envelopes for BUSHIPS Type II, N = 1.1 Sections Having a Camber Ratio of 0.04

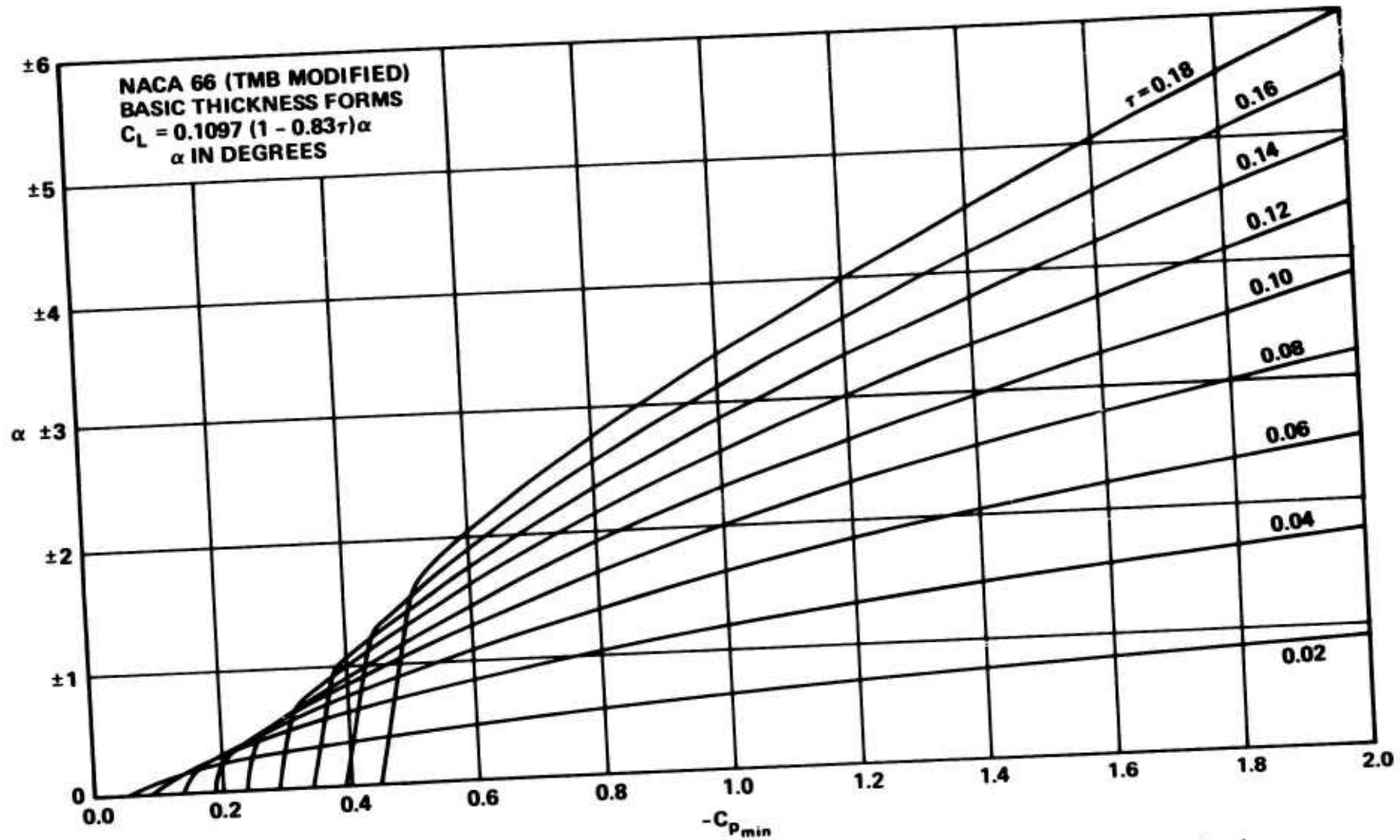

Figure 14 – Minimum Pressure Envelopes for NACA 66 (TMB Modified) N = 1.1 Sections with Zero Camber

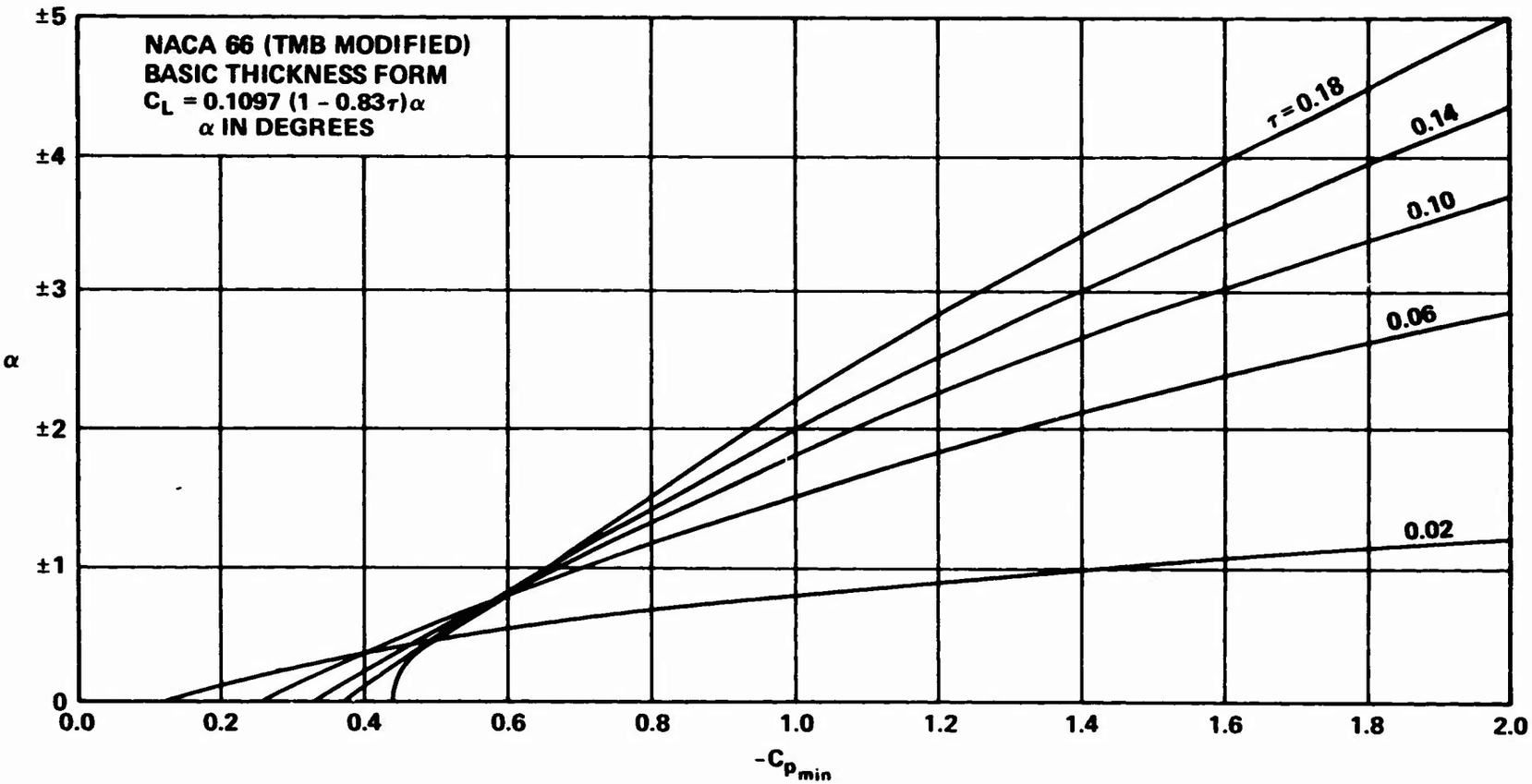

Figure 15 – Minimum Pressure Envelopes for NACA 66 (TMB Modified) N = 1.3 Sections with Zero Camber

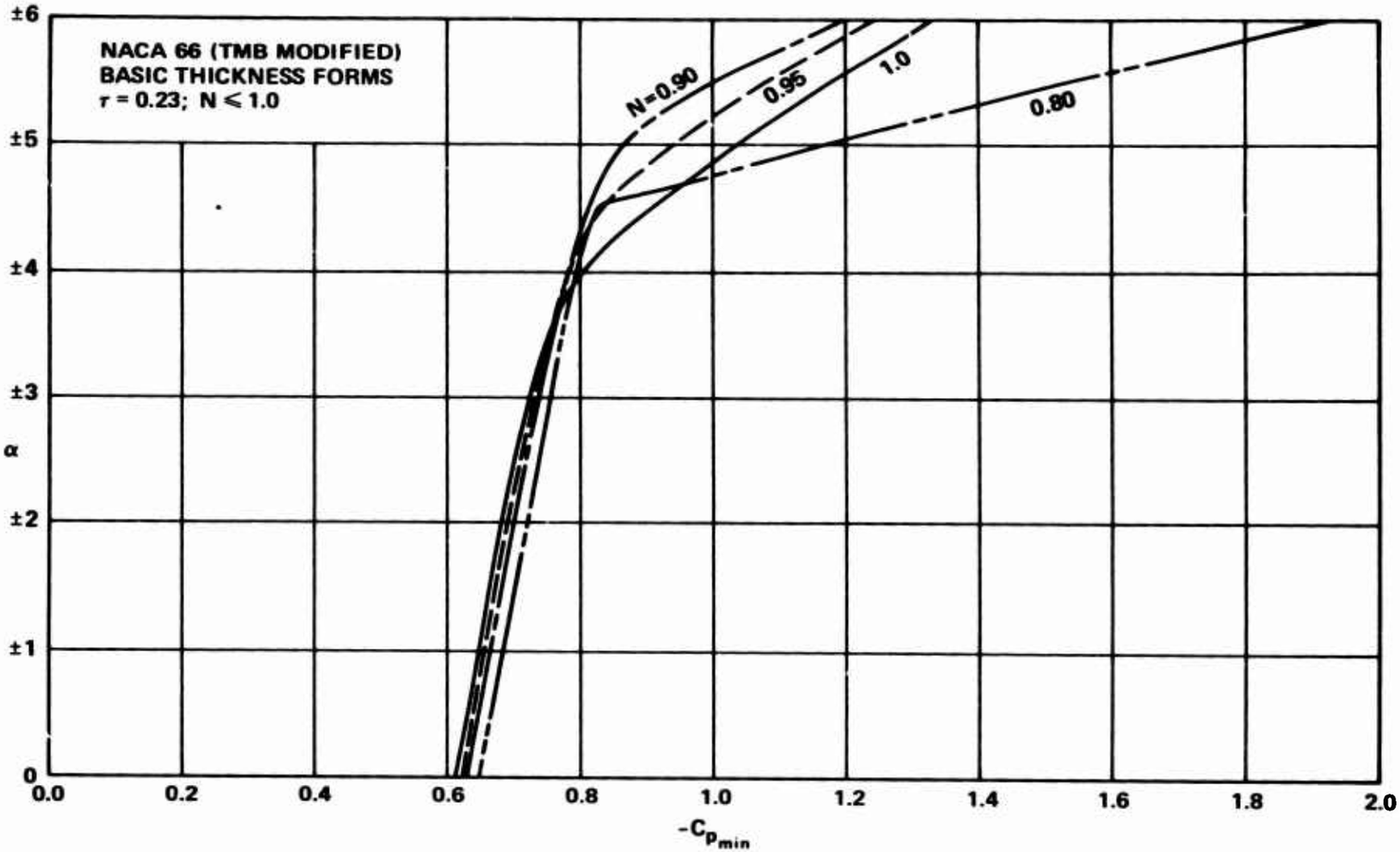

Figure 16 – Minimum Pressure Envelopes for NACA 66 (TMB Modified) N-Modified Sections; $N \leqslant 1.0$, $\tau = 0.23$ with Zero Camber

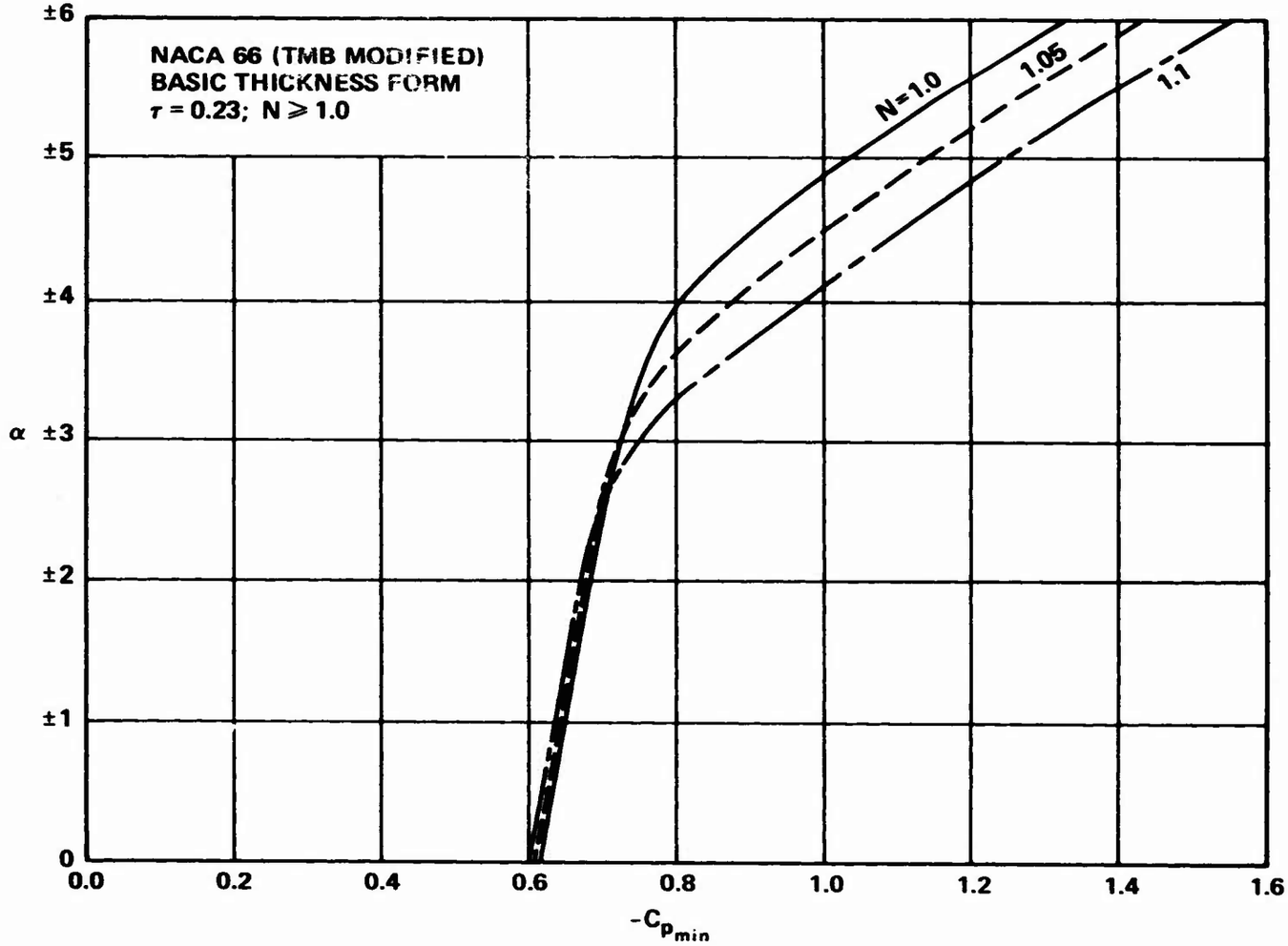

Figure 17 – Minimum Pressure Envelopes for NACA 66 (TMB Modified) N-Modified Sections: $N \geqslant 1.0$, $\tau = 0.23$ with Zero Camber

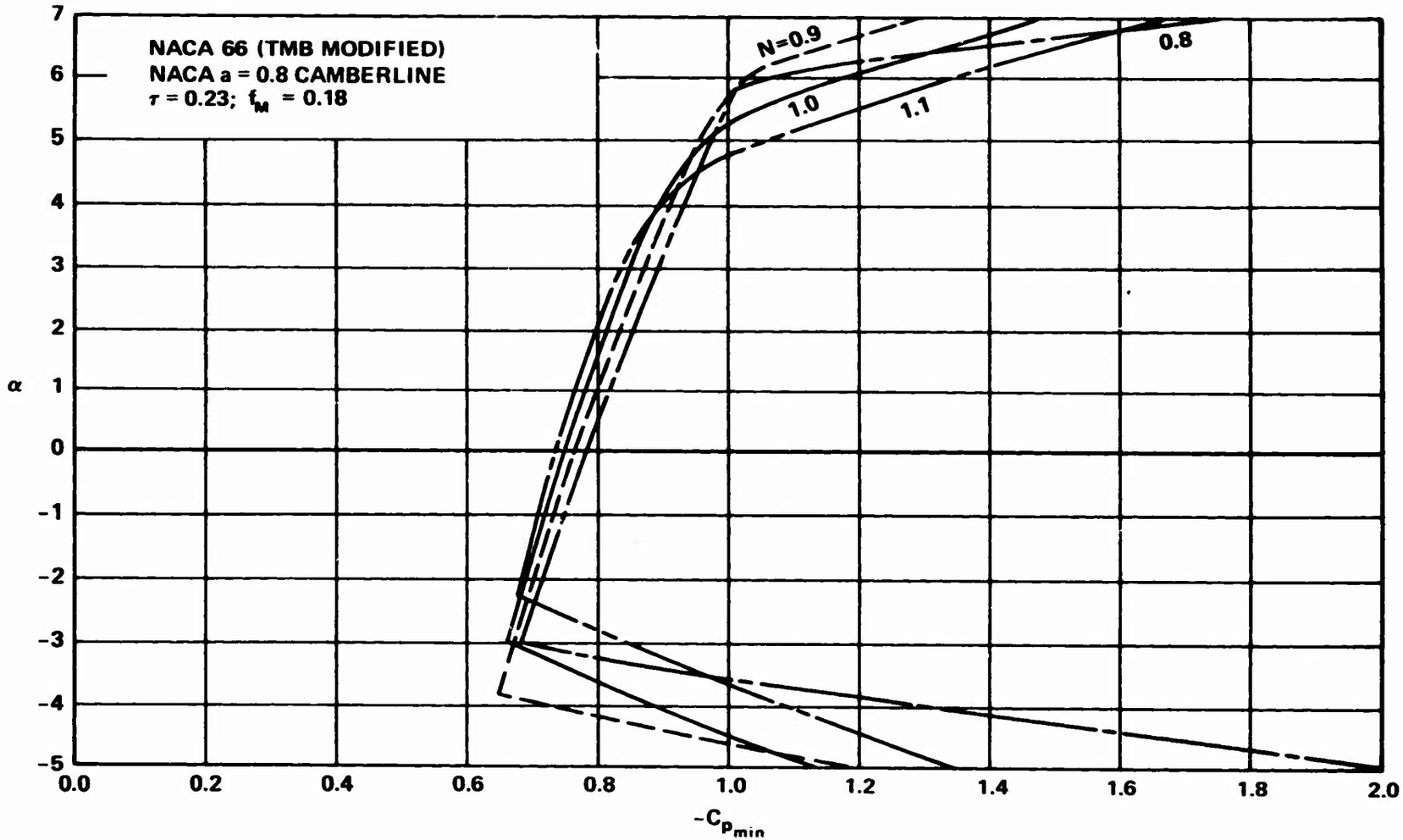

Figure 18 – Minimum Pressure Envelopes for NACA 66 (TMB Modified) N-Modified Sections; Range of N, $\tau = 0.23$, $f_M = 0.18$

angle-of-attack range can be realized. In this investigation this range was found to be within $0.8 < N < 1.3$. The maximum N is between 1.1 and 1.3 as mentioned previously, and the minimum N is between 0.8 and 0.9.

Figure 19 shows the inception characteristics for an ϵ modified method* combined with the BUSHIPS Type I hydrofoil. The ϵ parameters chosen were typical of several recently designed Navy propellers. The transformation equation for this modification is:

$$(Y_T/\tau)_{\epsilon_i} = [(1/2) - (\epsilon_i/\tau c)]2(Y_T/\tau)_{\epsilon_i=0} + (\epsilon_i/\tau c) \qquad (6)$$

where $i = 1, 2$ corresponds to the leading and trailing edges, respectively. The formulas results in an additional thickness of $2\epsilon_1$ at the leading edge and an additional thickness of $2\epsilon_2$ at the trailing edge. The maximum thickness and chord remain identical to the thickness and chord of the parent section, which in this example is the BUSHIPS Type I hydrofoil, an NACA 16 with a parabolic tail. The leading-edge radius for the foil (in this investigation) was determined by the computer-fairing technique in the vicinity of the leading edge as described in Brockett.[1] In this example the ϵ modified basic thickness form is defined as follows

$$\frac{\epsilon_1}{\tau c} = 0.05277$$

$$\frac{\epsilon_2}{\tau c} = 0.12550$$

Therefore, from the leading edge to the midchord

$$\left(\frac{Y_T}{\tau}\right)_{\epsilon_1} = 0.89446 \quad \left(\frac{Y_T}{\tau}\right)_{\epsilon_i=0} + 0.05277$$

and from the midchord to the trailing edge

$$\left(\frac{Y_T}{\tau}\right)_{\epsilon_2} = 0.7490 \quad \left(\frac{Y_T}{\tau}\right)_{\epsilon_i=0} + 0.12550$$

*Naval Ship Systems Command, "Propeller Blade Section Design Coefficients for Type I Sections," BUSHIPS Drawing 203-1737514 (21 Jul 1958).

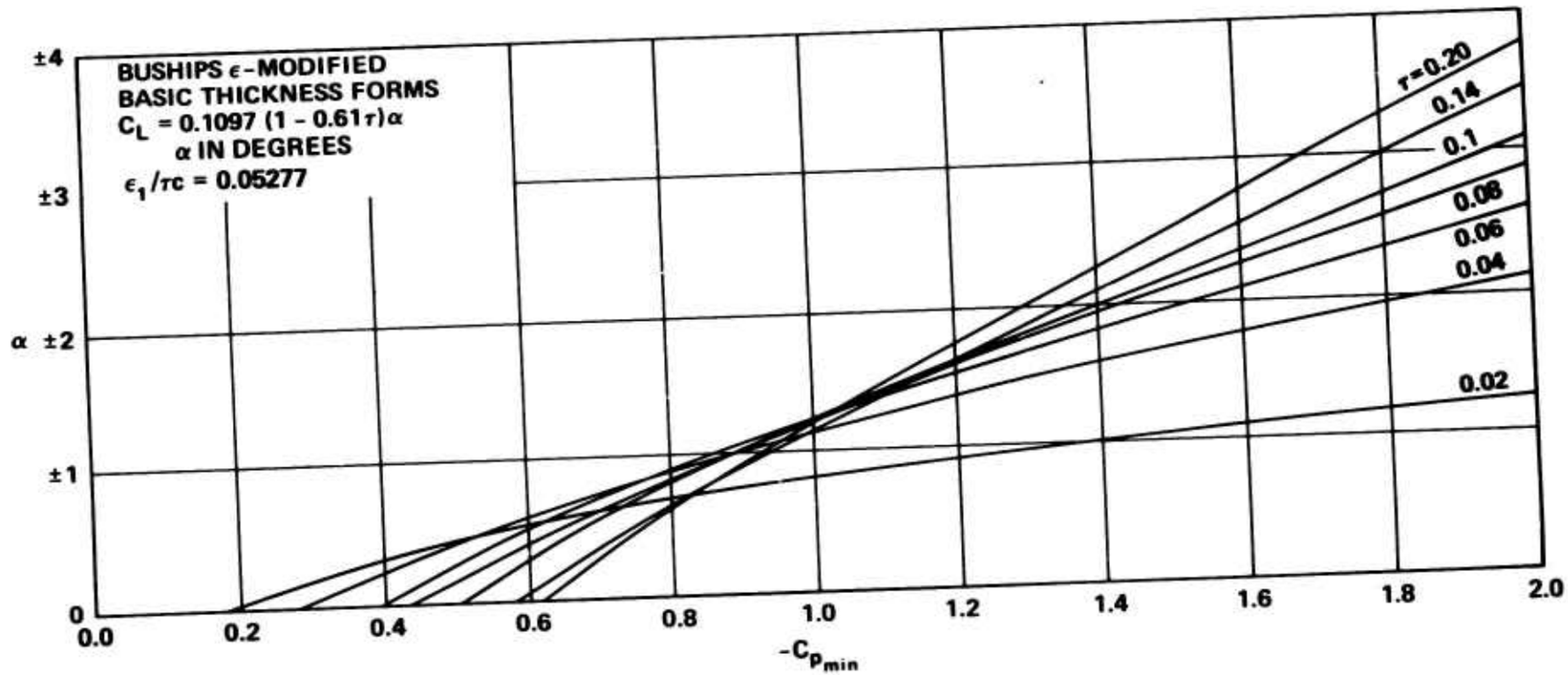

Figure 19 – Minimum Pressure Envelopes for BUSHIPS Type II, ϵ Modified Sections with Zero Camber

The leading-edge radius for this basic thickness form as determined from the computer output at zero angle of attack is given by

$$\rho_{LE} = 1.459\,\tau^2$$

From the previously described equations, the ϵ modified basic thickness form given in Table 2 was determined.

The data given in Figure 20 show that this design is not within the range of N's which gives beneficial effects. In fact, by comparing C_N for the ϵ modified design with C_N for the N-modified designs you would expect this to be the case; see Table 3.

DISCUSSION

To begin the discussion of nose radius effects on the cavitation characteristics of hydrofoils, one should first consider the inception characteristics of the parent hydrofoils predicted by Brockett; see Figures 1 through 6. His results show that as the nose radius increases with thickness ratio, the range of cavitation-free angle of attack increases. However, a decrease in shock-free inception speed must be accepted. By considering small modifications of the thickness distribution as a means of varying the nose radius, one might expect the same trends in the changes in the cavitation-inception curves of the hydrofoil. However, the present investigation has shown that this was not the case.

Figure 7 is a sketch of the cavitation inception characteristic for a typical basic thickness distribution of a propeller-type hydrofoil. The cavitation index σ_d and the critical cavitation index σ_c are not significantly different. For a given design cavitation index there is a unique thickness ratio for a given hydrofoil which gives the maximum cavitation-free angle of attack range δ. A plot of δ yields an outer envelope which for a given hydrofoil separates two zones, the cavitation zone in which cavitation is inevitable and the cavitation free zone in which a judicious choice of thickness ratio for a given camber and foil shape leads to a design that will not cavitate. For the foils considered in this investigation, the outer envelopes of the cavitation-free zone are compared in Figures 21 and 22. For small increases in nose radius, the range of cavitation-free angles of attack decreases, while for small decreases in nose radius, the range of cavitation-free angles of attack increases. This is opposite to the effect of increasing the thickness of the hydrofoil and is due to the different effects of each modification on the pressure distribution.

Increasing the thickness-to-chord ratio increases the suction in the vicinity of the midchord relative to the suction at the leading edge. Also, increasing the thickness-to-chord ratio increases the total suction for a given chordwise thickness distribution. These effects can be observed

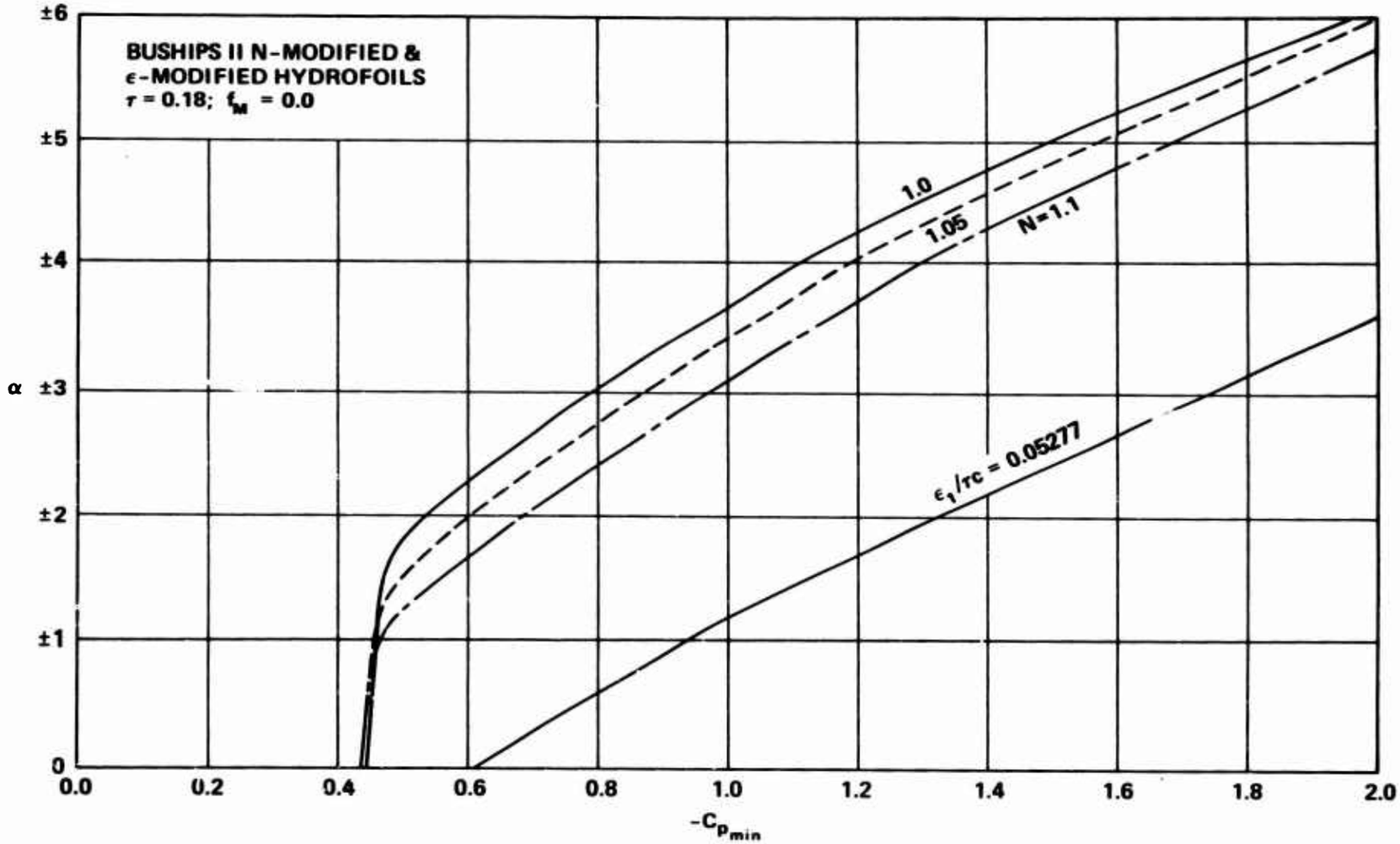

Figure 20 – Comparison of Cavitation Characteristics of BUSHIPS Type II, N-Modified and ϵ Modified Hydrofoils with $\tau = 0.18$ and Zero Camber

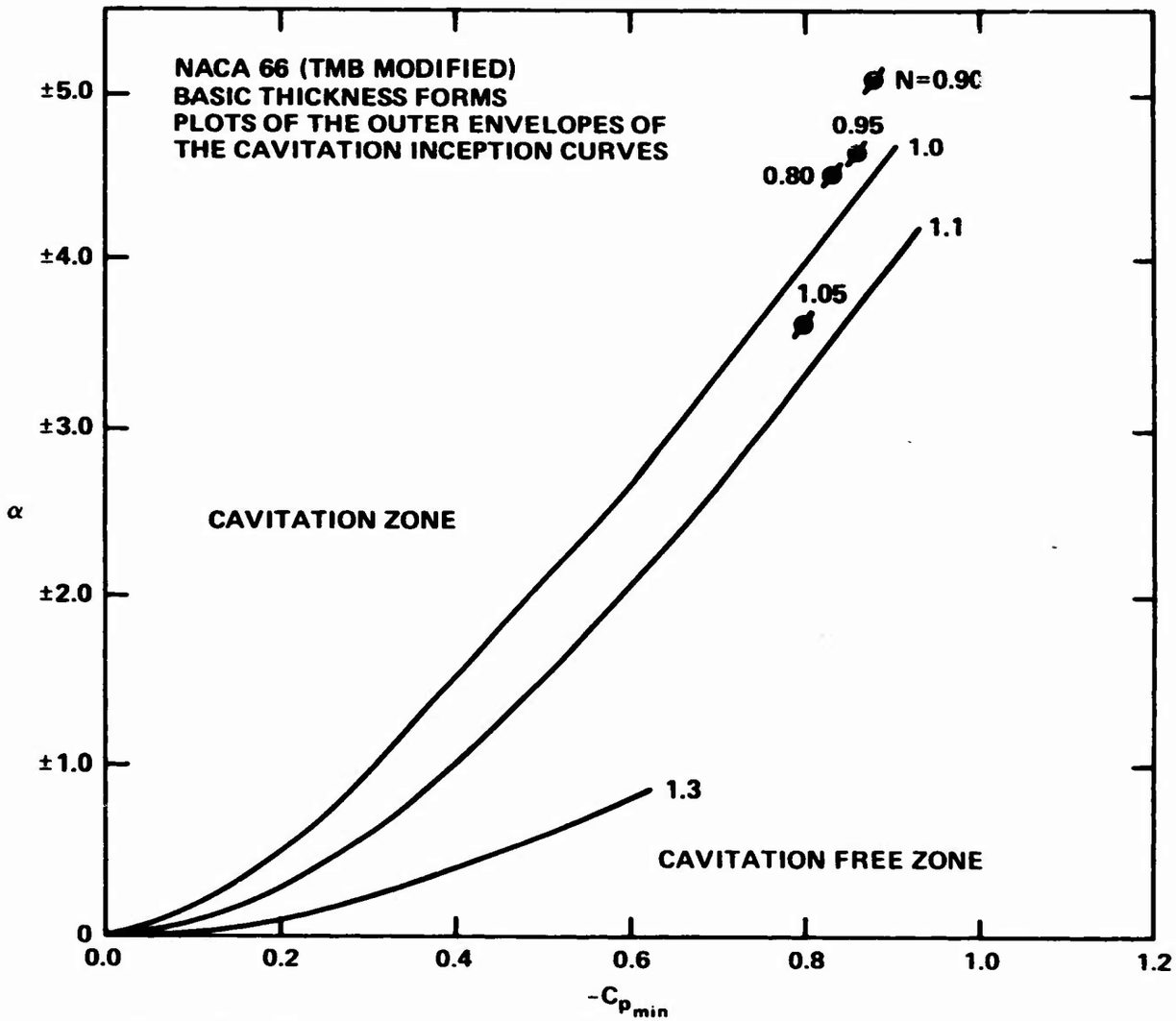

Figure 21 - Comparison of the Outer Boundary of the Minimum Pressure Envelopes of the NACA 66 (TMB Modified) N-Modified Sections with Zero Camber

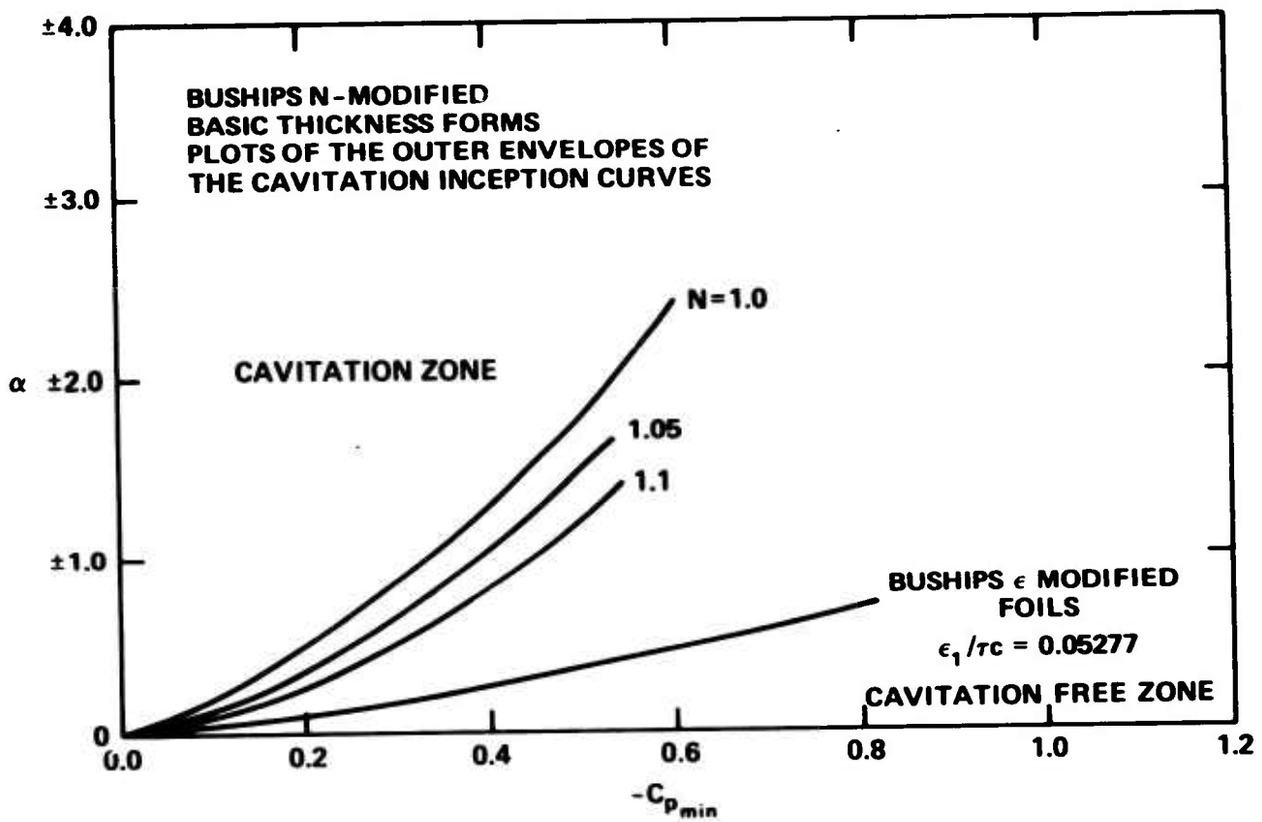

Figure 22 – Comparison of the Outer Boundary of the Minimum Pressure Envelopes of BUSHIPS Type II, N-Modified and ϵ Modified Sections with Zero Camber

by studying the pressure distributions given by Abbott and Von Doenhoff.[14] These results were consistent with the inception curves presented by Brockett.[2] The total increase in the suction for an increase in thickness-to-chord ratio explains the decrease in critical inception speed, i.e., the increase in critical σ_c; see Figures 1 through 6. Also, the decrease in leading-edge suction due to increasing thickness-to-chord ratio explains the increase in the range of cavitation-free angle of attack. This is because suction at the midchord increases at a slower rate than suction at the leading edge when angle of attack is increased.

Changing the nose radius while keeping the thickness-to-chord ratio constant, i.e., changing the leading-edge shape of the hydrofoil, has the opposite effect on the pressure distribution. Increasing the nose radius increases leading-edge suction while it decreases the midchord suction. This results in the increase in critical inception speed with a sacrifice of some of the range of cavitation-free angle of attack. The reverse occurs with decreases in the nose radius. These results are for small changes in nose radius about the parent hydrofoil geometry. Also, as pointed out before, only a small range of leading-edge changes results in beneficial effects on the cavitation-inception curves. The range of the leading-edge parameter N for which beneficial effects occur is within $0.8 < N < 1.3$ for the foil shapes considered.

DESIGN EXAMPLES

Three examples are presented to illustrate the usefulness of the results of this investigation. The first example illustrates a rational approach to the problem of increasing the thickness of the leading edge of a hydrofoil. A required increase in the leading-edge thickness has resulted in at least one design problem to date, viz., the introduction of air ducts in the vicinity of the leading edge of propeller-blade hydrofoils to emit air into the low-pressure region. The second example illustrates the improvement in cavitation inception gained by using a blunter hydrofoil, depending on the design criteria chosen, and assuming that small changes in the leading-edge geometry do not affect the hydrofoil lift curve slope and angle of zero lift. The third example illustrates the application of modifying the leading edge after cavitation experiments are conducted, and early inception of blade-surface cavitation seems to be a problem.

For the first example, consider the following situation. The decision has been made to use an air-emission system to introduce air at the low-pressure region of the leading edge of a propeller blade to minimize the effects of cavitation-associated problems. Assume the operating range of attack angle for the 0.7-radius blade element is $-1/2 < \alpha < 1/2$. If the BUSHIPS Type II hydrofoil with zero camber is chosen as the hydrofoil for this blade

[14] Abbott, I. H. and A. E. Von Doenhoff, "Theory of Wing Sections," Dover Publications, Inc., New York (1959).

element, to obtain the maximum cavitation-free range of operating pressure coefficients, the required thickness-to-chord ratio τ is 0.07; see Figure 1. Consequently, the cavitation-inception index for this design is approximately 0.20. However, assume that this foil is not blunt enough and that an $\epsilon_l / c\tau = 0.05277$ is required to accommodate the air ducts. From Figure 19, the ϵ type modification results in a cavitation-inception index of 0.63 for a $\tau = 0.07$. A second method for increasing thickness at the leading edge is to use the N = 1.1 modified hydrofoil data given in Figure 11. For $-1/2 < \alpha < 1/2$ and for the maximum cavitation-free range of minimum pressure coefficient, the thickness-to-chord ratio is 0.08 with a cavitation-inception index of 0.30. Table 4 gives these data along with giving the differences in the thickness at the 5-percent-chord location for a 36-inch chord. The table shows that if the BUSHIPS foil is inadequate because of size limitations, a better method for obtaining a thicker foil is to use the N-modified-foil data. The N = 1.1 modified hydrofoil yields a foil with more than adequate thickness in the vicinity of the leading edge, as well as a sacrifice of only 0.1 in the cavitation-inception index as opposed to a sacrifice of 0.43 in the cavitation-inception index for a sufficient increase in leading-edge thickness, using the ϵ modification method. Even if $\tau = 0.07$ was used for the BUSHIPS N = 1.1 foil, better cavitation performance as well as adequate thickness would be realized.

The second example is a design that requires a camber ratio of 0.02 for a BUSHIPS Type II hydrofoil. Suppose the maximum angle of attack α_t for this hydrofoil is +1 degree. For maximum cavitation-free speed, the N = 1.0 design requires a thickness-to-chord ratio of 0.06, which leads to $\sigma_i = 0.38$, and the greatest minimum cavitation-free angle of attack α_{-max} at $\sigma_i = 0.38$ is -0.6 degree; see Figure 2. For the maximum cavitation-free speed range, the N = 1.1 design requires $\tau = 0.08$, which leads to $\sigma_i = 0.4$ and $\alpha_{-max} = -0.55$ degree; see Figure 12. Utilizing a blunter foil to maximize the cavitation-free speed range leads to detrimental effects. However, suppose the operating cavitation index σ is 0.3, and that the avoidance of back bubble cavitation is desired. For the N = 1.0 case, $\tau = 0.04$ and $\sigma_i = 0.63$; for the N = 1.1 case, $\tau = 0.05$ and $\sigma_i = 0.5$; Table 5 gives the results. This example illustrates that when the avoidance of back bubble cavitation is the controlling factor and leading-edge cavitation is inevitable, the N = 1.1 slightly blunter hydrofoil is better, and, when the criteria is to maximize the range of cavitation-free speed, the sharper foil is better.

For the third example assume that the cavitation characteristics of a propeller or other control surface are to be evaluated experimentally in a water tunnel. Suppose cavitation is observed at the designed operating condition at two radial positions which are defined by NACA 66 (TMB modified) hydrofoils with a $\tau = 0.23$ and $f_M = 0$; $\tau = 0.23$ and $f_M = 0.18$, respectively. Assume that inception occurs at or near the designed cavitation index. Figures 16 through 18 show it is possible to modify the hydrofoil without changing the hydrodynamic performance significantly so as to improve cavitation characteristics. Figure 16 shows, for the

TABLE 4 – COMPARISON OF THICKENING METHODS

Hydrofoil	τ	σ_i	$(Y_T/\tau)_{5\%\ Chord}$	For c = 36" $t_{5\%\ Chord}$
BUSHIPS Type II	0.07*	0.20	0.20908	0.527"
ϵ Modified ($\epsilon_1/c\tau$ = 0.05277)	0.07	0.63	0.22633	0.570"
BUSHIPS N = 1.1	0.07	0.31	0.23189	0.584"
BUSHIPS N = 1.1	0.08*	0.30	0.23189	0.668"

*For maximum cavitation-free range of cavitation-inception indices.

TABLE 5 – HYDROFOIL DESIGN PROBLEM, COMPARING DIFFERENT FOIL CHOICES

f_M = 0.02 Cavitation Criteria	$\alpha_i = +1^\circ$ Foil of Choice	
	N = 1.0	N = 1.1
For Maximum Cavitation Free Speed	τ = 0.06 σ = 0.38 $\alpha_{-max} = -0.6^\circ$	τ = 0.08 σ = 0.4 $\alpha_{-max} = -0.55^\circ$
For σ = 0.3, Avoidance of Back Bubble and Inevitable Leading-Edge Cavitation	τ = 0.04 σ = 0.63 $\alpha_{-max_i} = -0.6^\circ$ $\alpha_{-max_o} = -0.35^\circ$	τ = 0.05 σ = 0.5 $\alpha_{-max_i} = -0.6^\circ$ $\alpha_{-max_o} = -0.35^\circ$

uncambered hydrofoil, that decreasing the leading-edge thickness slightly yields an increase in cavitation-free, angle-of-attack range in the vicinity of the designed cavitation index, along with a slight decrease in the shock-free-entry, cavitation-inception speed. Between N equal to 0.8 and 0.9 a minimum sharpening parameter exists; higher values of N yield new hydrofoils with progressively worse cavitation-inception characteristics. Also note that the relative divergence ψ of the inception characteristics (Figure 7) decreases with increasing sharpness of the leading edge. Therefore, the benefits realized are only in the vicinity of the design σ. Figure 17 shows, for the uncambered hydrofoil, that increasing the leading-edge thickness decreases the cavitation-free, angle-of-attack range about the design cavitation index, along with a slight increase in the cavitation-free, shock-free-entry range of speed. Similar effects result for the cambered hydrofoil as shown in Figure 18. The usefulness of these results can be illustrated as follows. Suppose intermittent leading-edge cavitation (flashing) is observed at the design cavitation index, which is assumed to be also the operating cavitation index. Sharpening the foil slightly would reduce or eliminate the amount of flashing cavitation as the hydrofoil passes through the flow nonuniformities, e.g., a propeller blade rotating in a wake.

CONCLUSIONS

The effect of varying the leading-edge radius of the NACA 66 (TMB modified) and BUSHIPS sections on the cavitation-inception characteristics was determined. The modification methods and the modified basic thickness forms were presented. For the hydrofoils considered the following can be said:

1. The NACA 66 (TMB modified) and BUSHIPS hydrofoil sections are good hydrofoil shapes for design purposes when cavitation suppression is desired on a hydrofoil section operating in a range of attack angles.

2. The range of N, the leading-edge radius parameter, for the NACA 66 (TMB modified) and BUSHIPS sections, which leads to slight deviations from the typical cavitation-inception characteristics was found to be within the range $0.8 < N < 1.3$. A limit to the increase in bluntness exists between N = 1.1 and 1.3. A limit to the increase in sharpness of the leading edge exists between N = 0.8 and 0.9.

3. Increasing the leading-edge radius, while keeping the maximum thickness and chord length constant, results in the development of a suction peak in the vicinity of the leading edge. The suction peak at midchord decreases with increase in the leading-edge radius.

4. Changing the leading-edge radius by changing the hydrofoil thickness indicates the possibilities of improving the cavitation-inception characteristics of propellers or other lifting surfaces, depending on the design criteria and the geometric constraints. One example showed that if back bubble cavitation suppression was the design criterion, a blunter foil would lead

to improved cavitation performance. It is well to note that each design problem is unique, and that the consideration and method of modification of the hydrofoil depends on the design problem.

5. The ϵ modified basic thickness form has cavitation characteristics which are not within the range of good shapes found in this investigation. A second design example has shown that a better method exists for increasing the leading-edge thickness without sacrificing a large loss in cavitation-inception speed.

RECOMMENDATIONS FOR FURTHER INVESTIGATION

1. Since possibilities exist with the modifications investigated for improving inception characteristics of fully wetted foils, the next logical step in this investigation is to plot similar inception curves for enough foils to obtain more easily usable design curves for the N-modified series. Thus, tradeoffs can be evaluated by the propeller designer to make a better choice of hydrofoil sections. However, before this undertaking, several modification methods should be investigated to determine the best modifying procedure. Subsequently, it would be desirable to develop an optimization computer program, having an optimum foil shape as its solution.

2. The results of this investigation indicate that only a limited range of fully wetted hydrofoil shapes exist that possess cavitation characteristics appropriate for propeller designs. Since the possibility exists for designing a base-vented hydrofoil, having better cavitation-inception characteristics than fully wetted hydrofoil designs at high speeds,[15] the wetted-surface inception characteristics of several base-vented section shapes should be determined.

---

[15] Lang, T. G., "Base-Vented Hydrofoils," Naval Ordnance Test Station, NAVORD Report 6606, China Lake, Calif. (19 Oct 1959).

REFERENCES

1. Brockett, T., "Steady Two-Dimensional Pressure Distributions on Arbitrary Profiles," David Taylor Model Basin Report 1821 (1965).

2. Brockett, T., "Minimum Pressure Envelopes for Modified NACA-66 Sections with NACA a = 0.8 Camber and BUSHIPS Type I and II Sections," David Taylor Model Basin Report 1780 (1966).

3. Eckhardt, M. K. and W. B. Morgan, "A Propeller Design Method," Society of Naval Architects and Marine Engineers Transactions, Vol. 63, pp. 325–374 (1955).

4. Milam, A. and W. B. Morgan, "Section Moduli and Incipient Cavitation Diagrams for a Number of NACA Sections," David Taylor Model Basin Report 1177 (1957).

5. Caster, E., "Incipient Cavitation Diagrams for BUSHIPS Type I and II Sections," David Taylor Model Basin Report 1643 (1962).

6. Morgan, W. B. and J. P. Lichtman, "Cavitation Effects on Marine Devices," Cavitation State of Knowledge published by American Society of Mechanical Engineers (Jun 1969).

7. Mandel, P., "Some Hydrodynamic Aspects of Appendage Design," Society of Naval Architects and Marine Engineers Transactions, Vol. 61, pp. 464–515 (1953).

8. Alef, W. E., "Propeller Sections to be Used in a Non-Homogeneous Wake," Hamburg Model Basin Report 1187 (Jun 1959).

9. Breslin, J. P. and L. Landweber, "A Manual for Calculation of Inception of Cavitation on Two and Three Dimensional Forms," Society of Naval Architects and Marine Engineers T & R Bulletin 1-21 (Oct 1961).

10. Berggren, R. E. and D. J. Graham, "Effects of Leading Edge Radius and Maximum Thickness-Chord Ratio on the Variation with Mach Number of the Aerodynamic Characteristics of Several NACA Airfoil Sections," National Advisory Committee for Aeronautics TN 3172 (1954).

11. Collins, I. F. and A. M. Evans, "Theoretical Study of the Cavitation Res[illegible]ice of Aerofoil Sections at Incidence," Admiralty Research Laboratory Report ARL/R4/G/AE/2/5 (Nov 1965).

12. Moeckel, G. P., "The Effect of Distortion of Subcavitating Foil Contours on Cavitation-Inception Velocity," Journal of Ship Research, pp. 253–262 (Dec 1966).

13. Pinkerton, R. M., "Effects of Nose Shape on the Characteristics of Symmetrical Airfoils," National Advisory Committee for Aeronautics TN 386 (Aug 1931).

14. Abbott, I. H. and A. E. Von Doenhoff, "Theory of Wing Sections," Dover Publications, Inc., New York (1959).

15. Lang, T. G., "Base-Vented Hydrofoils," Naval Ordnance Test Station, NAVORD Report 6606, China Lake, Calif. (19 Oct 1959).